



Structural Properties and Frequency Response Analysis of Simplified Water Quality Models: The Case of Time-Invariant Coefficients

Lewandowska, A.

IIASA Working Paper

WP-81-116

September 1981



Lewandowska, A. (1981) Structural Properties and Frequency Response Analysis of Simplified Water Quality Models: The Case of Time-Invariant Coefficients. IIASA Working Paper. WP-81-116 Copyright © 1981 by the author(s).
<http://pure.iiasa.ac.at/1645/>

Working Papers on work of the International Institute for Applied Systems Analysis receive only limited review. Views or opinions expressed herein do not necessarily represent those of the Institute, its National Member Organizations, or other organizations supporting the work. All rights reserved. Permission to make digital or hard copies of all or part of this work for personal or classroom use is granted without fee provided that copies are not made or distributed for profit or commercial advantage. All copies must bear this notice and the full citation on the first page. For other purposes, to republish, to post on servers or to redistribute to lists, permission must be sought by contacting repository@iiasa.ac.at

NOT FOR QUOTATION
WITHOUT PERMISSION
OF THE AUTHOR

STRUCTURAL PROPERTIES AND
FREQUENCY RESPONSE ANALYSIS
OF SIMPLIFIED WATER QUALITY
MODELS: THE CASE OF TIME-
INVARIANT COEFFICIENTS

A. Lewandowska

September 1981
WP-81-116

Working Papers are interim reports on work of the International Institute for Applied Systems Analysis and have received only limited review. Views or opinions expressed herein do not necessarily represent those of the Institute or of its National Member Organizations.

INTERNATIONAL INSTITUTE FOR APPLIED SYSTEMS ANALYSIS
A-2361 Laxenburg, Austria

PREFACE

In recent years there has been considerable interest in developing models for river and lake ecological systems, much of it directed towards large and complex simulation models. However, this trend has given rise to concern on several important counts, notably, for example, on methodological questions of model validity and credibility and in accounting for the effects of uncertainty. Task 2 of IIASA's Resources and Environment Area, on "Environmental Quality Control and Management", addresses problems such as these. One of the principal themes of the Task's work is to develop a framework for modeling poorly-defined environmental systems.

This paper re-assesses some properties of the classical advection-dispersion model for describing interactions between dissolved oxygen and biochemical oxygen demand concentrations in a reach of river. In particular, a frequency-domain approach is used for determining a sufficient accuracy for choosing approximate transformations of the classical model that are consistent with corresponding indexes of accuracy related to the field data available for model evaluation. The approach is illustrated for the case of the River Cam in eastern England (see also RR-78-19).

SUMMARY

This paper deals with the analysis of the structural properties of simplified river water quality models with time invariant coefficients. The structure of the simplified models should be chosen in such a way as to provide a satisfactory compromise between model accuracy and complexity.

The approach discussed here is based on an analysis of the dynamic properties of the system as well as on the frequency characteristics of the input signals. The analysis of the dynamical properties of the system has been performed for a one-dimensional (in space) time-invariant distributed-parameter model. The unsteady solutions for coupled, partial, differential equations (with two variables: DO and BOD concentrations) with time-invariant coefficients are considered. The model equations are transformed in a special way into diffusion equations, whose solution can be obtained by using the separation of variables method (SVM). As a result, a linear infinite order, ordinary differential equation system, with the same eigenvalues as those of the partial differential equations is obtained. The dynamical properties of the system are characterized here on the basis of a transmittance analysis as well as on the basis of a modal analysis (analysis of eigenfunctions).

The paper concludes with the possibility of choosing a simplified lumped-parameter (finite-order) dynamic or static model of water pollution, which ensures a compromise between accuracy and complexity of the model. It offers, in particular, answers to the following questions:

- what is the dimensionality of the simplified lumped-parameter model?
- what is the structure of this model?

The approach is illustrated with results from a case study of the River Cam in eastern England.

TABLE OF CONTENTS

1. INTRODUCTION	1
2. MATHEMATICAL MODEL	3
3. TRANSFORMATION OF MODEL EQUATIONS	7
4. DIFFUSION EQUATIONS WITH TIME INDEPENDENT COEFFICIENTS: THE SEPARATION OF VARIABLES METHOD	9
5. TRANSMITTANCE ANALYSIS	12
6. FREQUENCY ANALYSIS	16
7. NUMERICAL EXAMPLE	22
8. CRITERIA FOR MODEL COMPARISON	22
9. SIMULATION RESULTS	23
10. FREQUENCY ANALYSIS	38
APPENDIX	45
REFERENCES	50

STRUCTURAL PROPERTIES AND FREQUENCY RESPONSE
ANALYSIS OF SIMPLIFIED WATER QUALITY MODELS:
THE CASE OF TIME-INVARIANT COEFFICIENTS

A. Lewandowska

1. INTRODUCTION

One of the most important points to remember when designing a water quality monitoring system, is to formulate an adequate model of the pollutant distribution process. There are several such models, the most complex being in the form of coupled, partial differential equations, the simplest one being in the form of black-box models derived from, for example, a time-series analysis. Many of them have been examined in the literature on the subject (Rinaldi et al., 1979; Thomann, 1972; Beck, 1978, 1980; Vasiliev, 1979).

For practical applications, the following problem must be solved: what would be the optimal model in this context where "optimal" is understood in the sense of ensuring a compromise between accuracy and complexity? In this paper, a method for solving this problem is presented. This approach is based on a frequency response analysis of the system and the spectral distribution of the input disturbances acting on the system. Two

methods have been applied--the Laplace transform and modal analysis of the set of partial differential equations. On the basis of this investigation, it is possible to answer the following questions:

- is it necessary to apply a static model or a dynamic one?
- what is the dimensionality of the simplified, lumped parameter model?
- what is the structure of this model?

Let us examine also the role of the methodology presented here in system identification. Generally, there are two possible ways of identifying a model:

- the black-box approach, when it is only assumed that a general class of models can possibly be taken into account (for example, those with ordinary differential equations);
- the physical approach, where one starts with the analysis of physical phenomena.

Both approaches have some disadvantages. The first one has a large number of parameters that have to be estimated. In practice, one of the possible canonical forms have to be used and all the parameters in this canonical form must be estimated.

Very complex models--usually described in terms of partial differential equations (PDE), namely, distributed parameter systems (DPS)--are derived from an analysis of physical considerations. It is not a very easy task to solve these kinds of models and to estimate their parameters. It is possible, however, to utilize the information contained in these models. Usually they are characterized by a small number of

parameters--this number is small when compared to the number of unknown coefficients in canonical form, in a lumped parameter system (LPS). On the basis of some theoretical investigations, it is possible to show that the parameters in lumped model canonical form are not independent--they depend entirely on the parameters of the distributed model. In such a way, we obtain a kind of specialized canonical form--a set of ordinary differential equations (ODE) depending on a relatively small number of parameters. This kind of approach can be treated as structural analysis (or, a priori identification); it makes the identification process essentially simpler.

It is necessary to point out again, that as all the considerations are for a general model it is not necessary to know the values of the parameters at this stage of the investigation. The identification process is performed later, when a simplified model has been obtained (Figure 1).

2. MATHEMATICAL MODEL

Let us consider the linear, one-dimensional, distributed parameter dispersion model, with constant coefficients describing pollution propagation in a section of the river. This model has been considered in many publications (Rinaldi et al., 1979; Thomann, 1972; Vasiliev, 1979):

$$\frac{\partial s}{\partial t} = D_x \cdot \frac{\partial^2 s}{\partial x^2} - u \cdot \frac{\partial s}{\partial x} - k \cdot s \quad (1)$$

$$\frac{\partial c}{\partial t} = D_x \cdot \frac{\partial^2 c}{\partial x^2} - u \cdot \frac{\partial c}{\partial x} - k_{11} \cdot s - k_{12} \cdot c + k_{13} \quad (2)$$

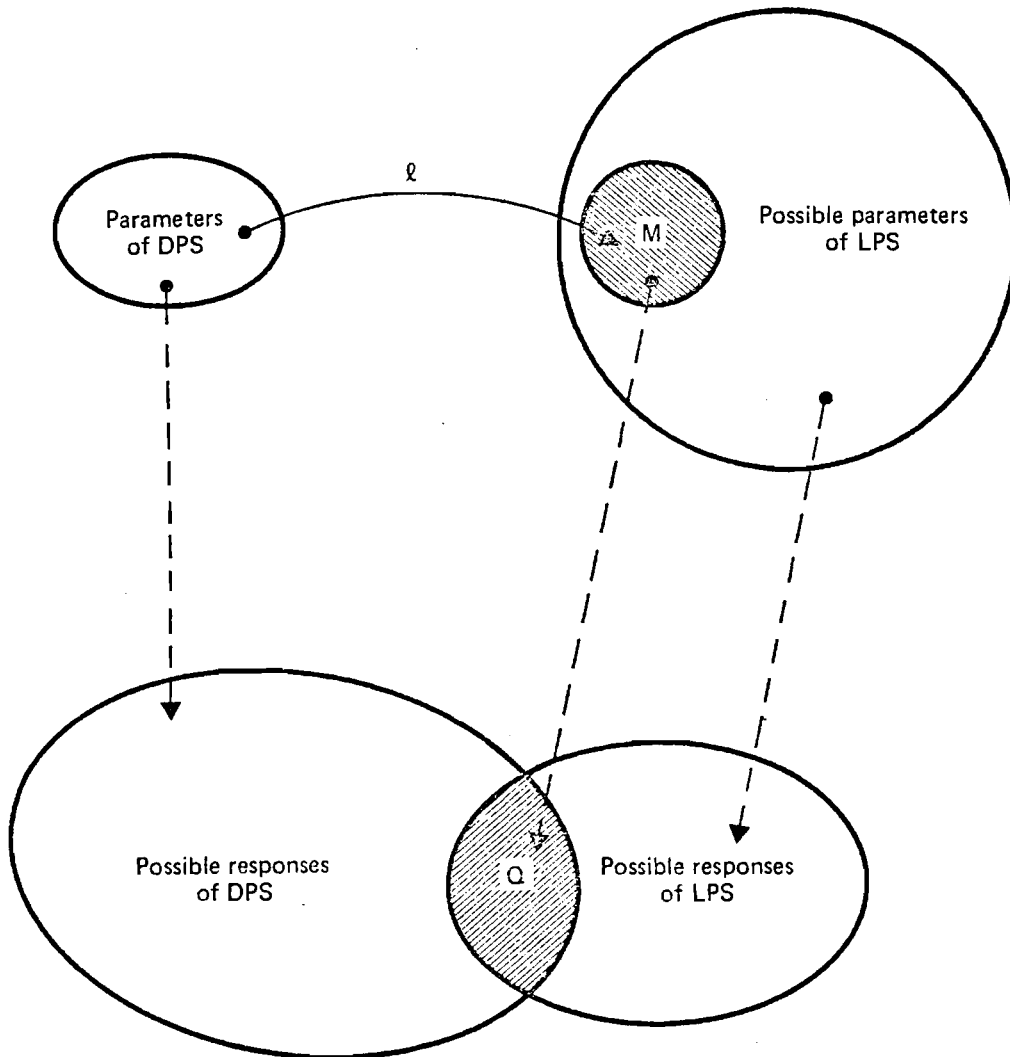


Figure 1. Schematic Synthesis of a Simplified Model
M - set of parameters depending on parameters of DPS obtained by transformation ϕ ,
Q - set of responses of the system obtained for parameters from M.

Comment: LPS has too many degrees of freedom, not all combinations of parameters are feasible. Only parameters in M should be taken into account during identification; transformation ϕ can be found a priori e.g. separation of variables method (SVM).

where

s is the pollutant concentration or value of BOD;
 c is the concentration of dissolved oxygen (DO);
 D_x is the longitudinal dispersion coefficient;
 u is the velocity of stream discharge along x-axis;
 $k, k_{11}, k_{12}, k_{13}$ are coefficients of linear approximation
of the function, which generally represents biochemical and oxygen reaction rates.

When making a comparison between equations (1), (2) and the Streeter-Phelps dispersion model (Rinaldi et al., 1979), it is easy to notice, that

k is the BOD decay coefficient,
 k_{12} the reaeration coefficient,
 k_{11} the deoxygenation coefficient,

$$k_{13} = k_{12} \cdot c_s + k_o$$

where c_s is the oxygen saturation concentration,

k_o the net rate of addition of DO to the reach due to effects other than those accounted for in the Streeter-Phelps model (in which $k_o = 0$). However, it is very easy to extend this model in order to consider the influence of solar radiation on algal growth and photosynthesis.

The assumptions concerning the linearity and the constant coefficients of the model are usually satisfied. It follows, that if we only consider short periods of time, we can assume time constant coefficients (the stream discharge and therefore, velocity u , can be constant in time). Similarly, the linear model can be used for small variations of pollution concentrations (it is a classical assumption in the case of linearization).

It is possible to consider the DO deficit instead of DO concentrations. It is not important for us however, what kind of state variables are used, because the relationship between concentration (c) and deficit (d) is very simple:

$$d = c_s - c \quad .$$

Therefore, the equations will have the same form in both cases. In the interests of simplicity, we also assume that the distributed sources and sinks are equal to zero.

Consider the boundary conditions for equations (1) and (2). In the case of a finite section of the river, two boundary conditions must be taken into account. However, because of the large influence of the convection terms $\frac{\partial s}{\partial x}$ and $\frac{\partial c}{\partial x}$ in equations (1) and (2) the role of the right boundary conditions for arriving at the solution can in practice be neglected. This means that we can assume any reasonable boundary condition, for example, equal to zero. The simplest way to define the boundary conditions is as follows:

$$s(0, t) = \psi_{1s}(t) \tag{3}$$

$$s(\ell, t) = 0 \tag{4}$$

$$c(0, t) = \psi_{1c}(t) \tag{5}$$

$$c(\ell, t) = 0 \tag{6}$$

where ℓ is the length of the river section.

These boundary conditions properly reflect the real situation--as usual, the point source of the pollutant is on the left side of the river segment. As was mentioned before, the boundary condition on the right side can be arbitrarily assumed.

To complete the problem formulation, we must consider the initial values for both state variables $s(x,t)$ and $c(x,t)$, if $t \in [0, t_f]$

$$s(x,0) = s_0(x) \quad x \in [0, l] \quad (7)$$

$$c(x,0) = c_0(x) \quad (8)$$

where $s_0(x), c_0(x)$ are the given functions.

3. TRANSFORMATION OF MODEL EQUATIONS

Our goal is to investigate the input-output behaviour of the system defined above. In order to simplify our work, we will introduce a useful transformation which eliminates the transportation term in equations (1) and (2). It is necessary to point out that this is only a formal operation without any physical meaning; moreover the same analysis can be performed without applying this transformation.

Let us consider the new state variables defined in the following way

$$\tilde{s}(x,t) = s(x,t) \cdot e^{-\alpha \cdot x} \quad (9)$$

$$\tilde{c}(x,t) = c(x,t) \cdot e^{-\alpha \cdot x} \quad (10)$$

where α is a parameter, $\alpha \in \mathbb{R}$.

By substituting equations (9), (10) for equations (1), (2) we obtain

$$\frac{\partial \tilde{s}}{\partial t} = D_x \cdot \frac{\partial^2 \tilde{s}}{\partial x^2} + (D_x \cdot 2 \cdot \alpha - u) \cdot \frac{\partial \tilde{s}}{\partial x} + (D_x \cdot \alpha^2 - u \cdot \alpha - k) \cdot \tilde{s} \quad (11)$$

$$\begin{aligned} \frac{\partial \tilde{c}}{\partial t} = & D_x \cdot \frac{\partial^2 \tilde{c}}{\partial x^2} + (D_x \cdot 2 \cdot \alpha - u) \cdot \frac{\partial \tilde{c}}{\partial x} + (D_x \cdot \alpha^2 - u \cdot \alpha - k_{12}) \cdot \tilde{c} + \\ & - k_{11} \cdot \tilde{s} + k_{13} \cdot e^{-\alpha \cdot x} \end{aligned} \quad (12)$$

It is possible to choose parameter α in such a way as to satisfy the equation

$$D_x \cdot 2 \cdot \hat{\alpha} - u = 0 \quad (13)$$

For the value $\hat{\alpha}$

$$\hat{\alpha} = \frac{u}{2 \cdot D_x} \quad (14)$$

equations (11), (12) can be reduced to a simpler form, without the convection term (first order derivative)

$$\frac{\partial \tilde{s}}{\partial t} = D_x \cdot \frac{\partial^2 \tilde{s}}{\partial x^2} - \left(\frac{u^2}{4 \cdot D_x} + k \right) \cdot \tilde{s} \quad (15)$$

$$\frac{\partial \tilde{c}}{\partial t} = D_x \cdot \frac{\partial^2 \tilde{c}}{\partial x^2} - \left(\frac{u^2}{4 \cdot D_x} + k_{12} \right) \cdot \tilde{c} - k_{11} \cdot \tilde{s} + k_{13} \cdot e^{-\hat{\alpha} \cdot x} \quad (16)$$

Let us denote

$$\beta_s = - \frac{u^2}{4 \cdot D_x} - k \quad (17)$$

$$\beta_c = - \frac{u^2}{4 \cdot D_x} - k_{12} \quad (18)$$

By comparing equations (15) and (16) with equations (17) and (18) we obtain the resulting system of equations:

$$\frac{\partial \tilde{s}}{\partial t} = D_x \cdot \frac{\partial^2 \tilde{s}}{\partial x^2} + \beta_s \cdot \tilde{s} \quad (19)$$

$$\frac{\partial \tilde{c}}{\partial t} = D_x \cdot \frac{\partial^2 \tilde{c}}{\partial x^2} + \beta_c \cdot \tilde{c} - k_{11} \cdot \tilde{s} + k_{13} \cdot e^{-\hat{\alpha} \cdot x} \quad (20)$$

It is necessary to point out that the transformation used does not change the boundary conditions (3)-(6).

4. DIFFUSION EQUATIONS WITH TIME INDEPENDENT COEFFICIENTS: THE SEPARATION OF VARIABLES METHOD

Consider equations (19) and (20) in the following form:

$$\frac{\partial \tilde{s}(x, t)}{\partial t} = D_x \cdot \frac{\partial^2 \tilde{s}(x, t)}{\partial x^2} + f_s(x, t) \quad (21)$$

$$\frac{\partial \tilde{c}(x, t)}{\partial t} = D_x \cdot \frac{\partial^2 \tilde{c}(x, t)}{\partial x^2} + f_c(x, t) \quad (22)$$

where

$$f_s(x, t) = \beta_s \cdot \tilde{s} \quad (23)$$

$$f_c(x, t) = \beta_c \cdot \tilde{c} - k_{11} \cdot \tilde{s} + k_{13} e^{-\hat{\alpha} \cdot x} \quad (24)$$

For the sake of generalization, we shall also consider the boundary conditions in the following form

$$\tilde{s}(0, t) = \psi_{1s}(t) \quad (25)$$

$$\tilde{s}(l, t) = \psi_{2s}(t) \quad (26)$$

$$\tilde{c}(0, t) = \psi_{1c}(t) \quad (27)$$

$$\tilde{c}(l, t) = \psi_{2c}(t) \quad (28)$$

Note, that the boundary conditions (3)-(6) are the particular cases of the ones above.

Let the initial conditions take the form

$$\tilde{s}(x, 0) = \phi_s(x) \quad (29)$$

$$\tilde{c}(x, 0) = \phi_c(x) \quad (30)$$

There are many possible techniques available to solve these equations. Our goal however is not to obtain a solution for specified boundary conditions but to analyze the input-output properties of the system. The separation of variables method (SVM) seems to be the best one for this purpose.

It is well known that it is possible to formulate the solution of these equations in the form of a Fourier series expansion based on eigenfunctions generated by the corresponding Sturm-Liouville operator (Porter, 1966):

$$\tilde{s}(x, t) = \sum_{m=1}^{\infty} T_{sn}(t) \cdot \sin\left(\frac{n\pi x}{\ell}\right) \quad (31)$$

$$\tilde{c}(x, t) = \sum_{m=1}^{\infty} T_{cn}(t) \cdot \sin\left(\frac{n\pi x}{\ell}\right) \quad (32)$$

where the expansion coefficients are

$$T_{sn}(t) = \frac{2}{\ell} \int_0^{\ell} \tilde{s}(x, t) \cdot \sin\left(\frac{n\pi x}{\ell}\right) dx \quad (33)$$

$$T_{cn}(t) = \frac{2}{\ell} \int_0^{\ell} \tilde{c}(x, t) \cdot \sin\left(\frac{n\pi x}{\ell}\right) dx \quad (34)$$

for $n = 1, 2, \dots$.

By integrating equations (33) and (34) in two stages, we obtain ordinary differential equations (see Appendix).

$$\begin{aligned} \frac{d}{dt} T_{sn}(t) + \left(\frac{n\pi}{\ell}\right)^2 \cdot D_x \cdot T_{sn}(t) &= \frac{2n \cdot \pi \cdot D_x}{\ell^2} [\psi_{1s}(t) - (-1)^n \cdot \psi_{2s}(t)] + \\ &+ f_{sn}(t) \end{aligned} \quad (35)$$

$$\begin{aligned} \frac{d}{dt} T_{cn}(t) + \left(\frac{n\pi}{\ell}\right)^2 \cdot D_x \cdot T_{cn}(t) &= \frac{2n \cdot \pi \cdot D_x}{\ell^2} [\psi_{1c}(t) - (-1)^n \cdot \psi_{2c}(t)] + \\ &+ f_{cn}(t) \end{aligned} \quad (36)$$

where

$$f_{sn}(t) = \frac{2}{\ell} \int_0^{\ell} \beta_s \cdot \tilde{s}(x,t) \cdot \sin\left(\frac{n\pi x}{\ell}\right) dx \quad (37)$$

$$f_{cn}(t) = \frac{2}{\ell} \int_0^{\ell} [\beta_c \cdot \tilde{c}(x,t) - k_{11} \cdot \tilde{s}(x,t) + k_{13} \cdot e^{-\alpha x}] \cdot \sin\left(\frac{n\pi x}{\ell}\right) dx \quad (38)$$

for $n = 1, 2, \dots$

Taking into account equations (33) and (34) and the time-independence of the coefficients in equations (21) and (22), we obtain

$$f_{sn}(t) = \beta_s \cdot T_{sn}(t) \quad (39)$$

$$f_{cn}(t) = \beta_c \cdot T_{cn}(t) - k_{11} \cdot T_{sn}(t) + k_{13} \cdot \frac{2n \cdot \Pi [1 - e^{-\alpha \cdot \ell} (-1)^n]}{[(\alpha \cdot \ell)^2 + (n\pi)^2]} \quad (40)$$

for $n=1, 2, \dots$,

where the term with k_{13} is the n -th coefficient of the expansion of $e^{-\alpha x}$ in the eigenfunctions basis. By substituting equations (39) and (40) into equations (35) and (36) we obtain

$$\begin{aligned} \frac{d}{dt} T_{sn}(t) + \left[\left(\frac{n\pi}{\ell}\right)^2 \cdot D_x - \beta_s\right] \cdot T_{sn}(t) &= \frac{2n \cdot \Pi \cdot D_x}{\ell^2} \\ &\cdot [\psi_{1s}(t) - (-1)^n \cdot \psi_{2s}(t)] \end{aligned} \quad (41)$$

$$\begin{aligned} \frac{d}{dt} T_{cn}(t) + \left[\left(\frac{n\pi}{\ell}\right)^2 \cdot D_x - \beta_c\right] \cdot T_{cn}(t) &= \frac{2n \cdot \Pi \cdot D_x}{\ell^2} \cdot [\psi_{1c}(t) - (-1)^n \cdot \psi_{2c}(t)] \\ - k_{11} \cdot T_{sn}(t) + k_{13} \cdot \frac{2n\pi [1 - e^{-\alpha \cdot \ell} (-1)^n]}{(\alpha \cdot \ell)^2 + (n\pi)^2} & \end{aligned} \quad (42)$$

for $n=1, 2, \dots$

The initial conditions for equations (41) and (42) can be obtained in a similar way

$$T_{sn}(0) = \frac{2}{\ell} \int_0^{\ell} \phi_s(x) \cdot \sin\left(\frac{n\pi x}{\ell}\right) dx \quad (43)$$

$$T_{cn}(0) = \frac{2}{\ell} \int_0^{\ell} \phi_c(x) \cdot \sin\left(\frac{n\pi x}{\ell}\right) dx \quad (44)$$

for $n=1,2,\dots$

5. TRANSMITTANCE ANALYSIS

During the previous stages of our investigations, we obtained an infinite-dimensional set of ordinary differential equations that were strictly equivalent to the original partial differential equations. One difficult problem arises here; for purely technical reasons, we are not able to handle an infinite set of equations and we must truncate the series (31) and (32). This, however, enables the construction of a simplified model, since it is sufficient to consider only a finite dimensional set of differential equations, which is in fact a truncated subset of equations (41) and (42). The only crucial point is how best to choose the length N of the truncated series. This number should be chosen as a compromise between the accuracy of the simplified model and the related computational effort. Since the assumptions deal with time-independence system coefficients, it is possible to propose a more constructive approach for solving this problem. This approach utilizes a frequency domain analysis of the system.

For the sake of simplicity, we will consider only the influence of the left boundary conditions (i.e., the input, upstream disturbances), and we will take zero initial values. Due to the linearity

of the system equations, we can omit the influence of the term containing k_{13} and that part of the solution which relates to the initial values. The superposition theorem holds true in this case, since those components of the solution that relate to these terms are not important from the point of view of the transmittance properties of the system.

Now, we can compute the transmittances between inputs (boundary conditions $\psi_{1s}(t)$, $\psi_{1c}(t)$) and state variables (expansion coefficients $T_{sn}(t)$, $T_{cn}(t)$, $n = 1, 2, \dots, N$).

$$G_{sn}(p) = \frac{k_{sn}}{1 + p \cdot \theta_{sn}} \quad (45)$$

$$G_{cn}^I(p) = \frac{k_{cn}^I}{1 + p \cdot \theta_{cn}} \quad (46)$$

$n = 1, 2, \dots, N$, p is the complex variable.

It is possible to observe that equations (41) and (42) are coupled by the distributed forcing function $f_{cn}(t)$; for this reason, we should consider two types of dynamic blocks G_{sn} , G_{cn} (two types of denominators).

The structure of the system can be represented using the block-scheme formalism (Figure 2). Parameters of the individual blocks have the following values:

- gain coefficients

$$k_{sn} = \frac{2n \cdot \Pi \cdot D_x}{\lambda^2} \theta_{sn} \quad (47)$$

$$k_{cn}^I = \frac{2n \cdot \Pi \cdot D_x}{\lambda^2} \theta_{cn} \quad (48)$$

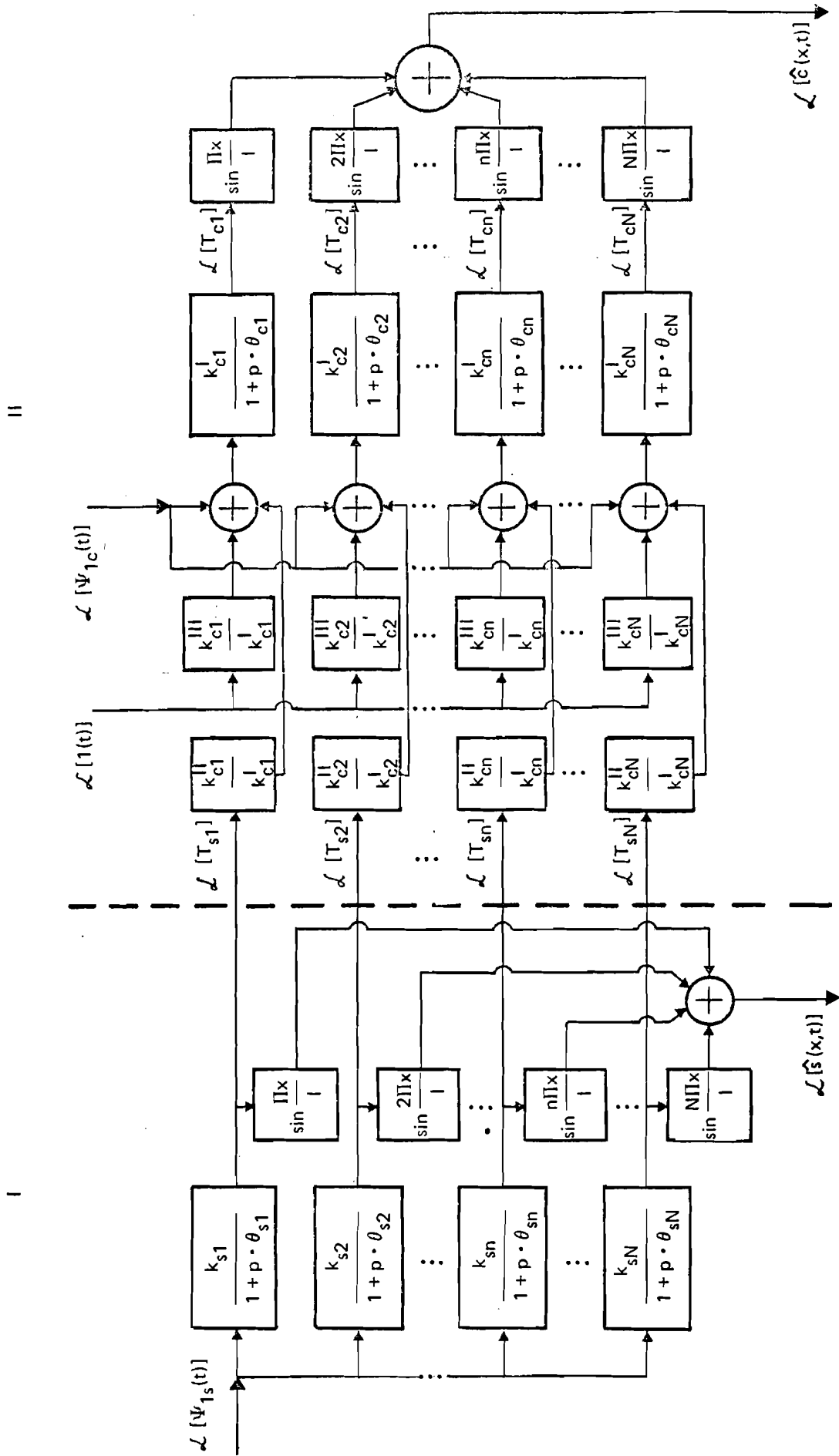


Figure 2. The Simplified Model Block Diagram (Dynamic Part)

$$k_{cn}^{II} = -k_{11} \cdot \theta_{cn} \quad (49)$$

$$k_{cn}^{III} = k_{13} \cdot \frac{2n\pi [1 - e^{-\hat{\alpha} \cdot \ell} (-1)^n]}{(\hat{\alpha} \cdot \ell)^2 + (n\pi)^2} \cdot \theta_{cn} \quad (50)$$

and time constants:

$$\theta_{sn} = \frac{1}{\beta_s - \left(\frac{n\pi}{\ell}\right)^2 \cdot D_x} \quad (51)$$

$$\theta_{cn} = \frac{1}{\beta_c - \left(\frac{n\pi}{\ell}\right)^2 \cdot D_x} \quad (52)$$

It is easy to compute the poles of the above transmittances

$$p_{sn} = \beta_s - \left(\frac{n\pi}{\ell}\right)^2 \cdot D_x \quad (53)$$

$$p_{cn} = \beta_c - \left(\frac{n\pi}{\ell}\right)^2 \cdot D_x \quad (54)$$

where β_s , β_c are determined by equations (17) and (18).

Laplace transforms the output signals, which approximate that solutions of equations (21) and (22) are equal

$$\mathcal{L}[\hat{s}(x_1, t)] = \sum_{n=1}^N \mathcal{L}[T_{sn}(t)] \cdot \sin\left(\frac{n\pi x}{\ell}\right) \quad (55)$$

$$\mathcal{L}[\hat{c}(x_1, t)] = \sum_{n=1}^N \mathcal{L}[T_{cn}(t)] \cdot \sin\left(\frac{n\pi x}{\ell}\right) \quad (56)$$

6. FREQUENCY ANALYSIS

In the previous sections of this paper, we have determined the transmittances describing the system dynamics. Our goal will now be to use these results to formulate the simplified model. This can be achieved by an analysis of the model's frequency response properties.

Each dynamic block in Figure 2 is, in fact, a low frequency filter, with frequency characteristics as shown in Figure 3. On the other hand, every signal acting in a real system has a finite frequency band - or can be approximated by a finite frequency band signal. This means that it is possible to determine a limited frequency f_g , with a property such, that all (or almost all) the signal energy is contained in this frequency band. In practice, this frequency can be obtained by applying spectral analysis methods and Fourier series techniques (see, e.g., Jenkins and Watts, 1968). It is interesting to compare the two frequencies, f_g (signal frequency band), and f_p , the frequency corresponding to the first pole of the system, where

$$\omega_p = 2\pi f_p = \min_{n=1,2,\dots,N} \{ |P_{sn}|, |P_{cn}| \} \quad (57)$$

Only two cases are interesting:

$$f_g \gg f_p \quad .$$

This means that the signal frequency band is so narrow that we can neglect the dynamic behaviour of the system. In this case, we can consider a static model as sufficiently accurate. It is necessary to expect, however, that this situation will not occur very often. The second case is for

$$f_p < f_g \quad .$$

In this case, the dynamic properties of the system should be taken into account. It is possible to observe however, that

the characteristic frequency of system transmittances G_{sn} , G_{cn} increases when n increases. It follows that N is such that

$$f_g < f_{pn}$$

where

$$\omega_{pn} = 2\pi f_{pn} = \{ |p_{sn}| \text{ or } |p_{cn}| \} \quad . \quad (58)$$

This means that all dynamic blocks with transmittances $G_{sn}(p)$ and $G_{cn}(p)$ can be treated as static blocks, if $n > N$. These inertia (dynamic) terms can be replaced by the proportional terms

$$G_{sn}(p) \cong k_{sn} \quad (59)$$

$$G_{cn}(p) \cong k_{cn}^I \quad . \quad (60)$$

Now, we can compute the sums

$$k_s(x) = \sum_{n=N+1}^{\infty} k_{sn} \cdot \sin\left(\frac{n\pi x}{\ell}\right) \quad (61)$$

$$k_c(x) = \sum_{n=N+1}^{\infty} k_{cn}^I \cdot \sin\left(\frac{n\pi x}{\ell}\right) \quad (62)$$

and consider the simplified model as shown in Figures 4 and 5.

It is necessary to point out that the best approximation of the original system has thus been obtained--best in the sense that the eigenvalues of the lumped parameter system are the same as the eigenvalues of the distributed parameter system. From this, it follows that the frequency and time responses of the approximate system will match well the responses of the original system. This cannot be expected for other approaches, for example, that presented by Rinaldi et al., (1979). There is very poor correspondence between the poles obtained in

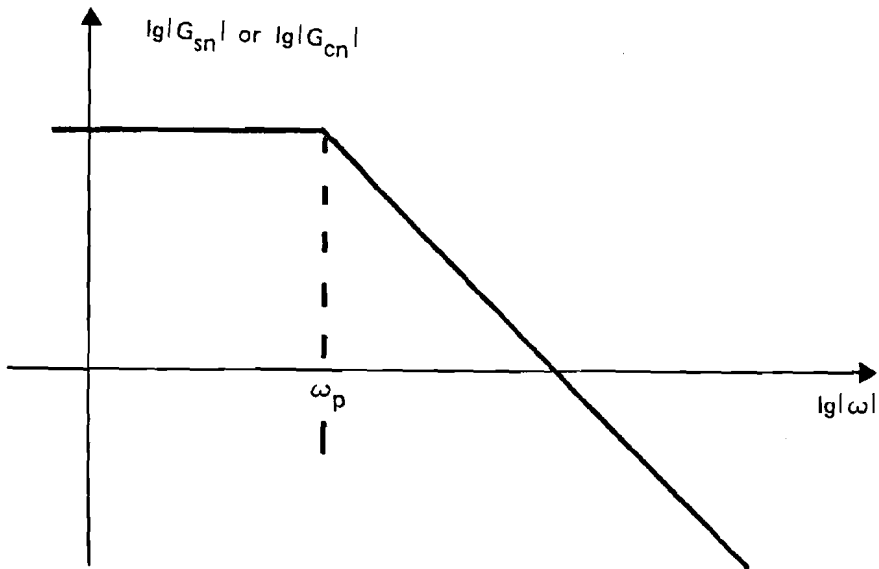


Figure 3. Asymptotic Frequency Characteristic of the Inertia Term

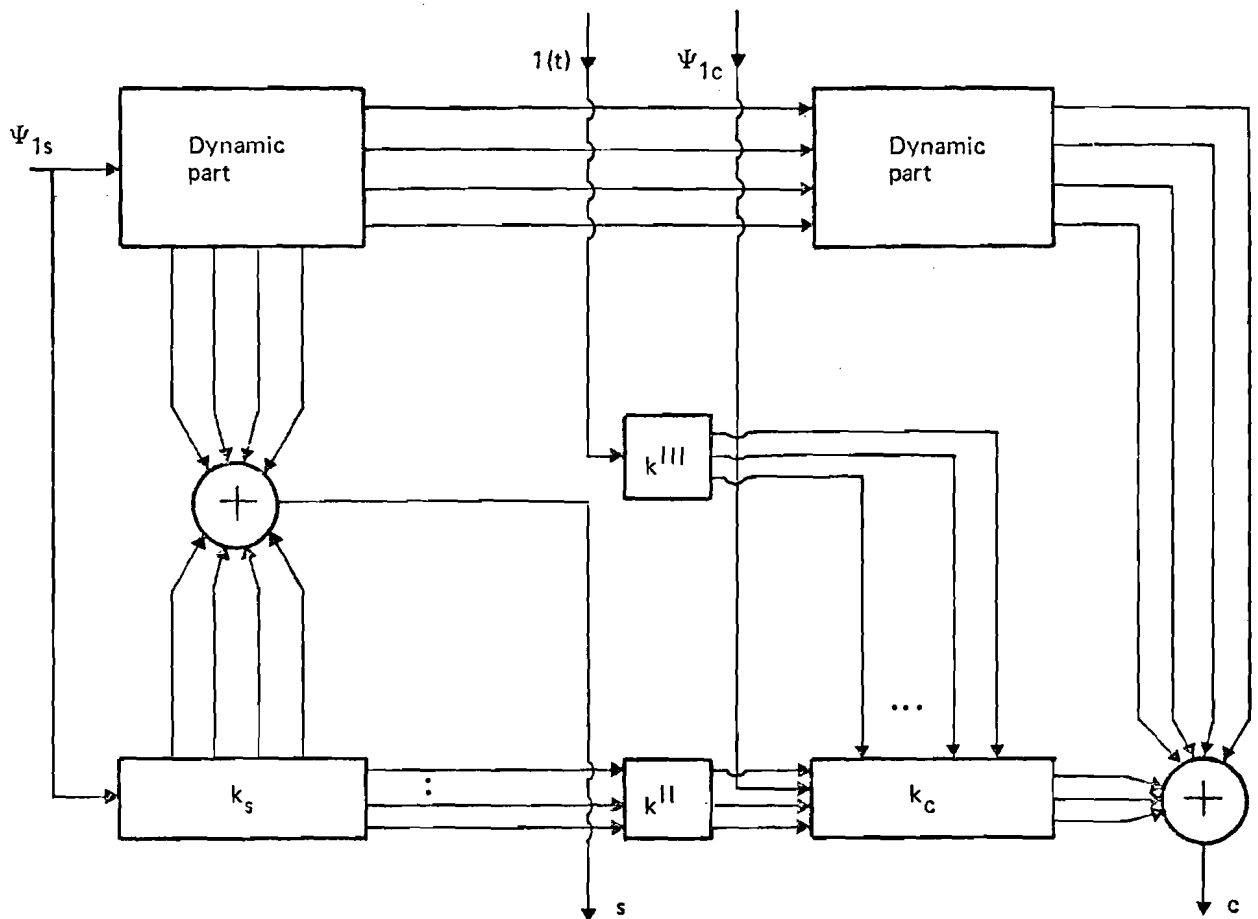


Figure 4. Structure of the Simplified Model

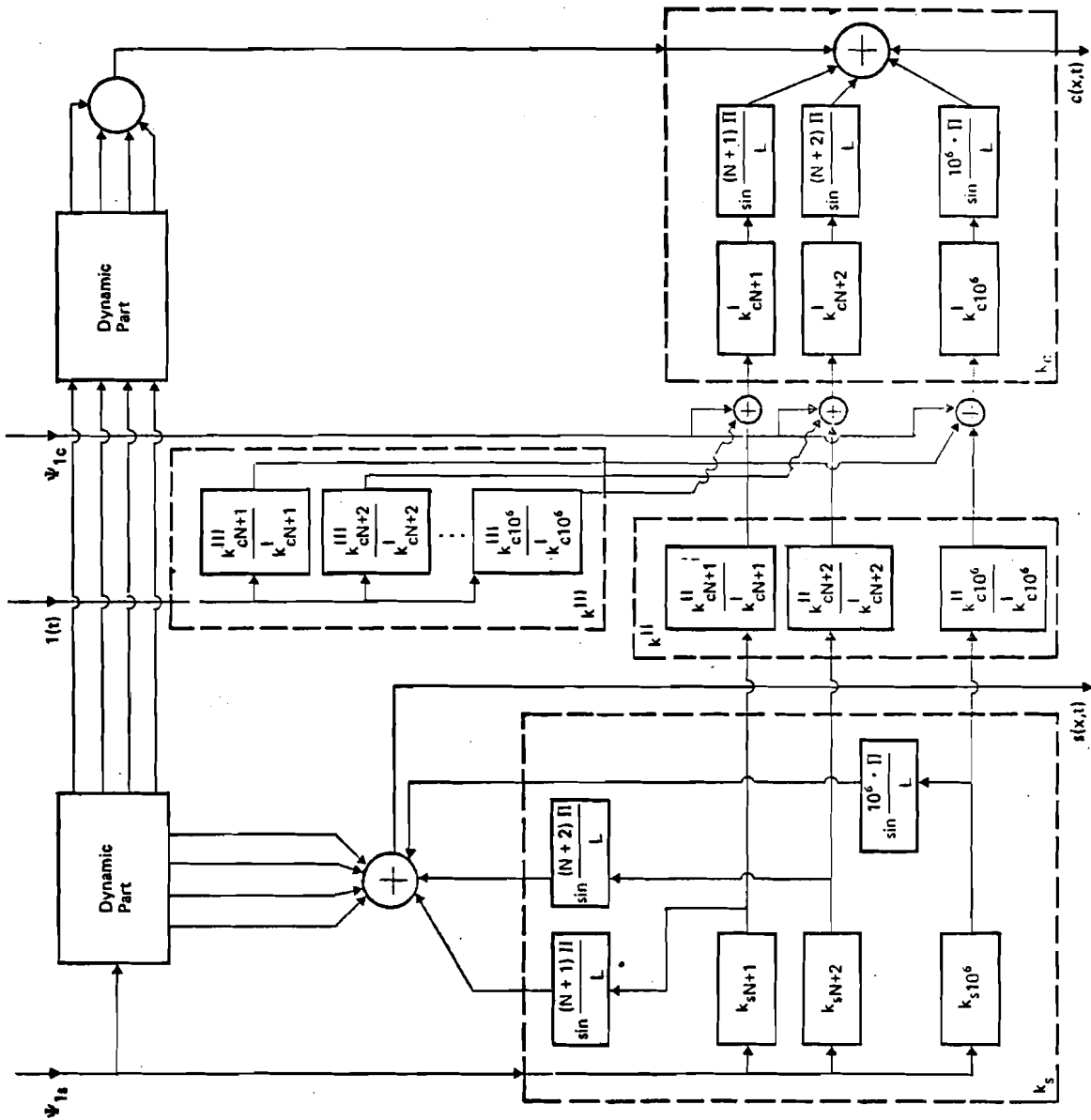


Figure 5. The Simplified Model (Block Diagram)

Rinaldi's work and the poles of the DPS model obtained in this paper. It would be an interesting exercise to compare the frequency characteristics obtained for both approaches.

The above results can be utilized in two ways: to analyze the qualitative properties of the system and to build a simplified computer model of the process considered.

It would be interesting to analyze more specifically the formula describing the poles of the system:

$$p_{sn} = - \frac{u^2}{4 \cdot D_x} - k - \left(\frac{n \cdot \Pi}{\ell} \right)^2 \cdot D_x \quad (63)$$

$$p_{cn} = - \frac{u^2}{4 \cdot D_x} - k_{12} - \left(\frac{n \cdot \Pi}{\ell} \right) \cdot D_x \quad (64)$$

in order to investigate the influence of the diffusion coefficient D_x on system behaviour. It is necessary to point out, however, that the above formula cannot be utilized for studying the limit behaviour when D_x tends to zero. This follows from the fact that the partial differential equations change in this case and therefore further investigations of this case should be carried out.

It is possible to utilize the present approach to build a computer model of the process. The only problem, however, is concerned with the properties of the Fourier series, because computing the sum of a Fourier series is an ill-defined process (see Tikhonov and Arsenin, 1977). On the other hand, the system eigenfunctions are equal to zero at both ends or boundaries of the interval. For these reasons, the value of ℓ should be determined in an appropriate way (Figure 6) and special methods should be applied to compute the sum of the Fourier series.

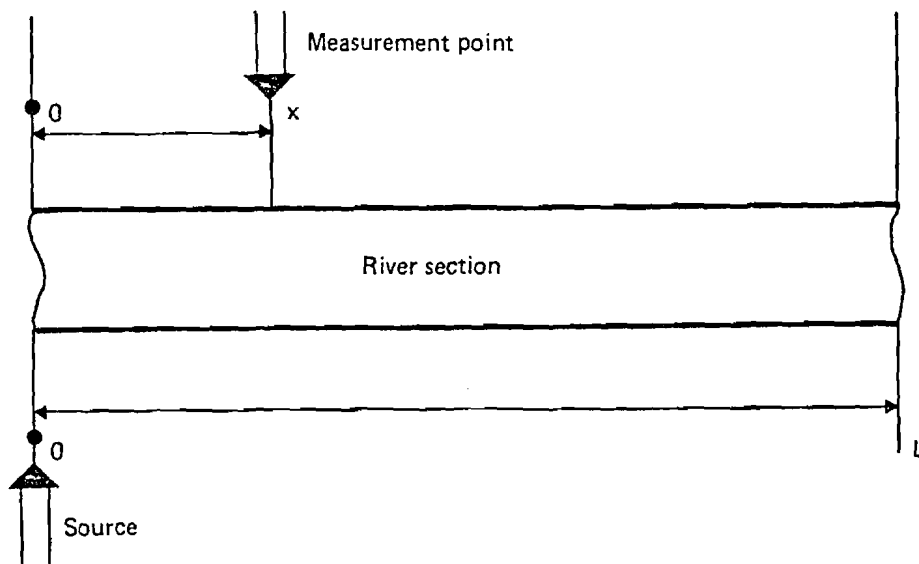


Figure 6. Schematic Definition of the River Section

7. NUMERICAL EXAMPLE

The simplified model presented in the previous section was utilized to describe the distribution of pollutants in a section of the river Cam, with the input point at Bait's Bite lock and the output point at Bottisham lock (see Beck, 1978). This model was used to predict DO and BOD concentrations at the measurement point 4.5 km distant from the source (see Figure 6). The parameter values assumed for the model are shown in Table 1. It is easy to notice that these parameter values are the same as those in Model I (in Beck's paper, 1978) except for k_{13} , the value of which in Beck's Model I, is equal to -1.0 for $t \leq t_{19}$ and $+1.0$ for $t > t_{19}$. (The influence of this difference is apparent when comparing the plot of DO output in Model I of Beck's paper (1978) with the plot of the simplified model's DO output as shown in Figure 14.) DO and BOD concentrations measured at Bait's Bite lock and at Bottisham lock, once daily through a 3-month period (see Beck, 1978) were taken as the input and the output signals.

8. CRITERIA FOR MODEL COMPARISON

It is one of the most important and difficult problems to find adequate criteria for the comparison of models. A number of possible approaches exist (see Raibman, 1975). Here the mean value and mean square of the residuals are considered. These values have been normalized, using average and mean square values of the system's outputs.

Table 1. Model Parameter Values

Parameter	Definition	Value
V	Volumetric hold up in the reach	$1.51 \cdot 10^5 \text{ m}^3$
Q	Average stream discharge	$1.28 \cdot 10^5 \text{ m}^3/\text{day}$
A	Average rectangular cross section	30.20 m^2
U	Average velocity of discharge along x-axis	4228 m/day
k_{12}	Reaeration rate coefficient	0.17 1/day
$k = k_{11}$	BOD decay coefficient	0.32 1/day
k_{13}	$k_{13} = k_{12} \cdot C_s + k_o$	$1.0 \frac{\text{mg}}{\ell \cdot \text{day}}$

9. SIMULATION RESULTS

The most interesting questions deal with the dimensionality of the simplified model, the length of the river section and the value for the dispersion coefficient. The simulation experiments were performed in two stages.

1. Assuming the dimensionality of the simplified model is equal to 1, the simulation experiments were repeated with different values for the length of the river section and for the dispersion coefficient. The mean square of the residuals (normalized by using process mean square) as a function of the dispersion coefficient for a fixed value of the river section length, is shown in Figures 7, 8 and 9. The same quality index of the model, as a function of the river section length and fixed values for

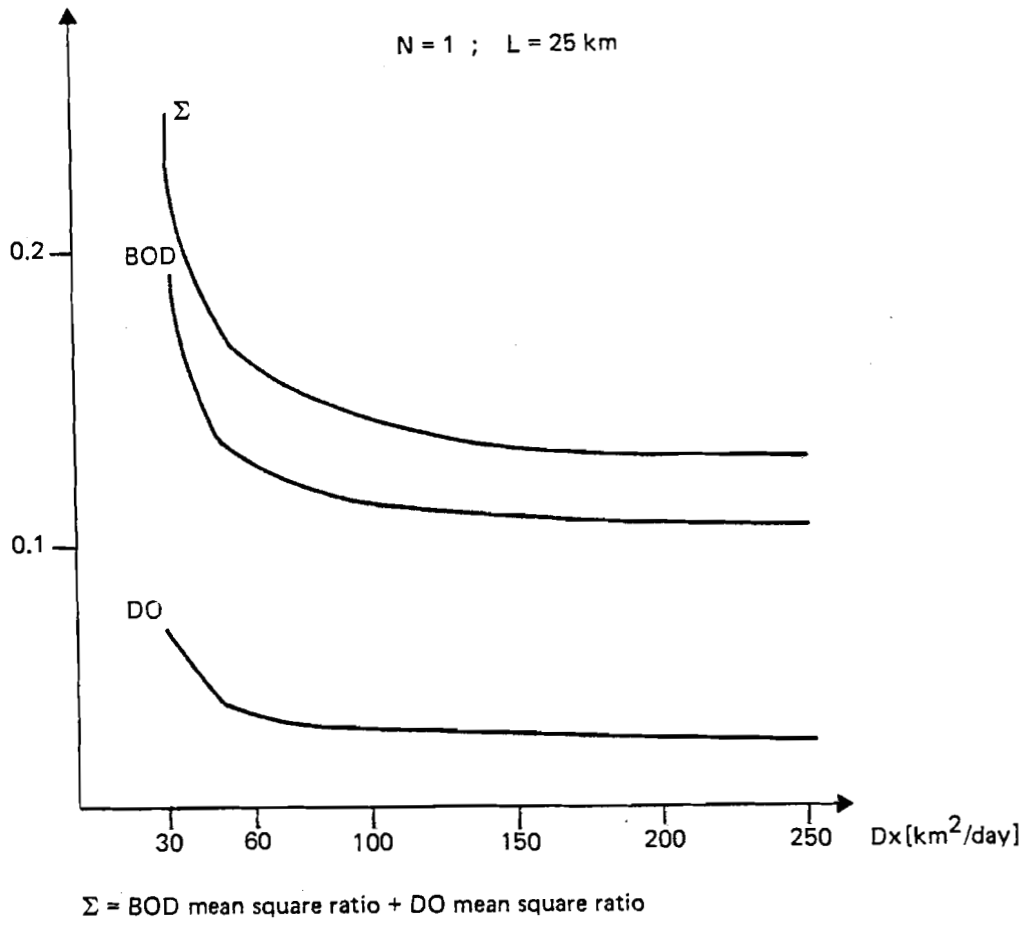


Figure 7. Quality Indexes for River Cam, N-1, L=25 km.

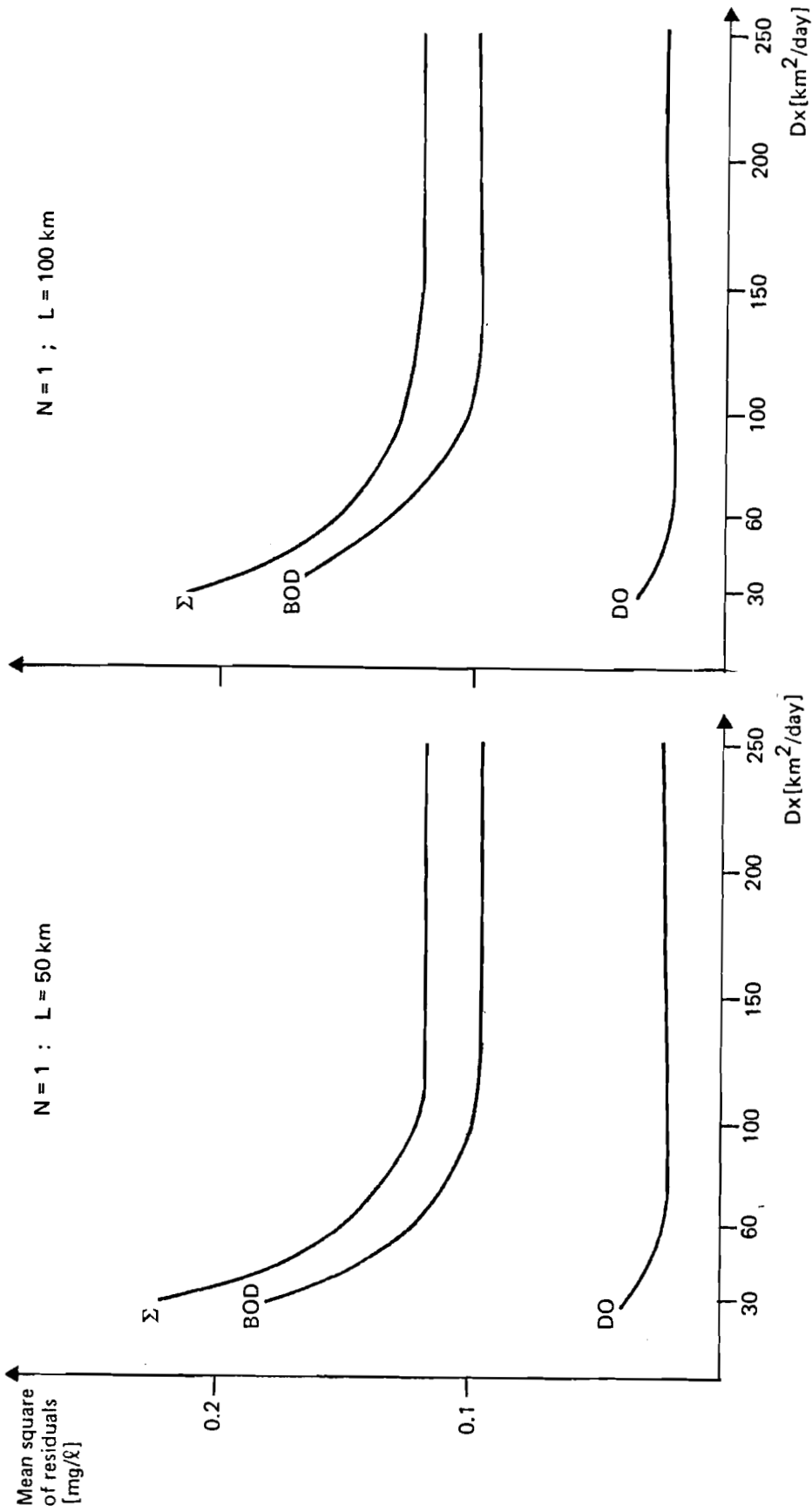


Figure 8. Quality Indexes for River Cam, N=1, L=50 km and L=100 km.

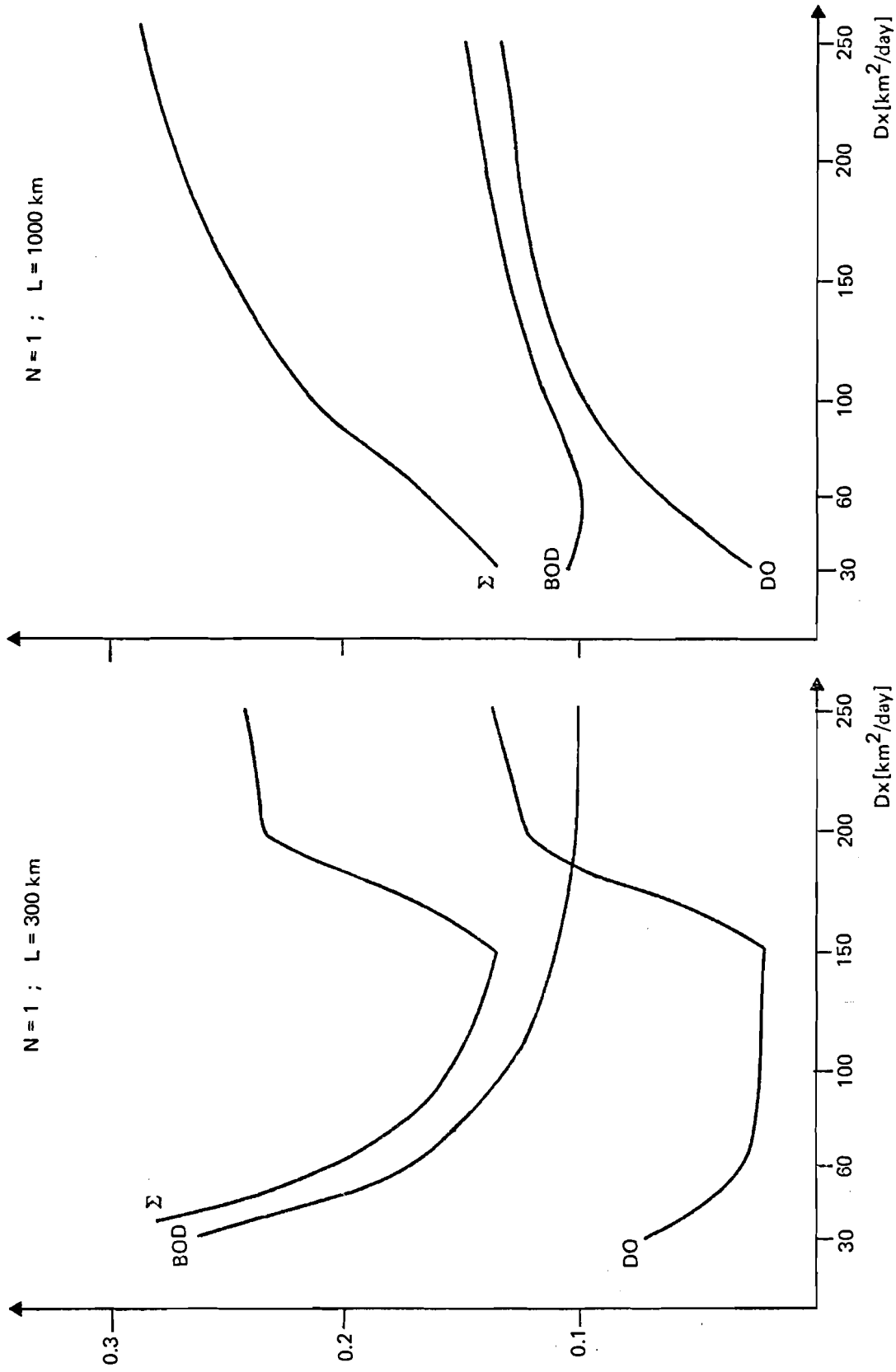


Figure 9. Quality Indexes for River Cam, $N=1$, $L=300 \text{ km}$ and $L=1000 \text{ km}$.

the dispersion coefficient, is shown in Figures 10, 11, and 12. From Figures 10, 11, and 12, it is easy to see that the smallest values for quality indexes have been obtained for a chosen length of the river section equal to 50 km. From Figures 9, 10, 11, and 12, one can conclude that, assuming the length ℓ to be larger than 100 km, the fit of the model is significantly worse. From Figures 7 and 8 it is easy to conclude that for $D_x > 100 \text{ km}^2/\text{day}$ the values of the quality indexes are almost constant (the curves being very flat).

2. Assuming the length $\ell = 50 \text{ km}$ and $\ell = 100 \text{ km}$ and various values for the dispersion coefficient D_x , simulation experiments were repeated for fixed dimensionalities of the model equal to 2 and 5. The results are presented in Figure 13.

From a comparison of the simulation results obtained, it follows that the best fit of the simplified model for the system is given by a value for the dispersion coefficient of $100 \text{ km}^2/\text{day}$, when we assume the river section length to be 50 km. These results have been obtained again for various other dimensionalities as well (Table 2).

It can be seen from Table 2 that for various dimensionalities of the simplified model, the quality indexes of these models have almost the same values. The significant conclusion is that a one-dimensional model is in fact sufficiently accurate. The output plots for the best case are shown in Figure 14.

It should be noted that the resulting value of the river section length of 50 km is a consequence of the compromise between two effects; (a) the error inherent in the Fourier method, and (b) the influence of the right boundary condition, which has been assumed to be equal to zero.

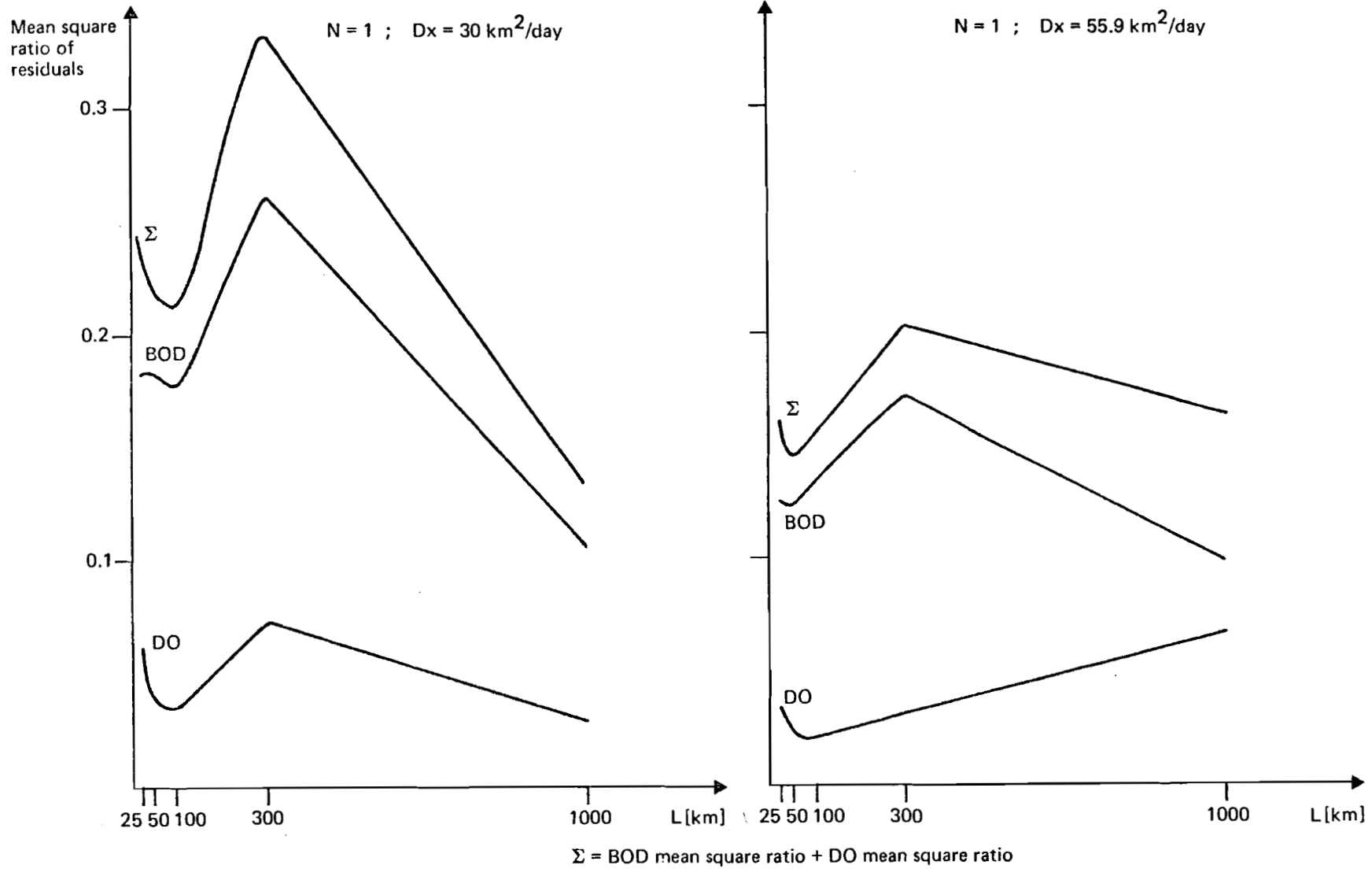


Figure 10. Quality Indexes for River Cam, $N=1$, $D_x=30 \text{ km}^2/\text{day}$ and $D_x=55.9 \text{ km}^2/\text{day}$.

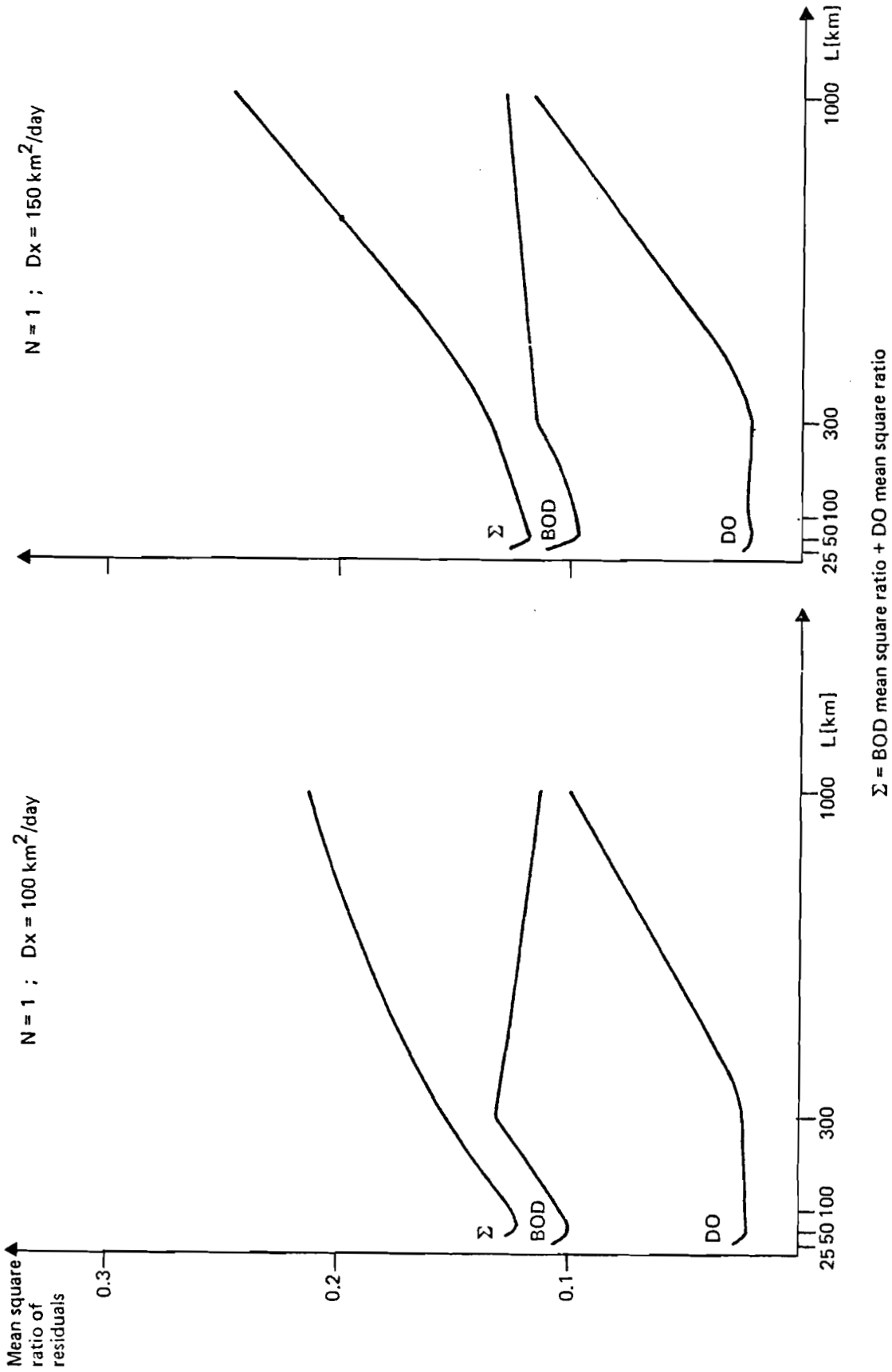


Figure 11. Quality Indexes for the River Cam, $N=1$, $D_x=100 \text{ km}^2/\text{day}$ and $D_x=150 \text{ km}^2/\text{day}$.

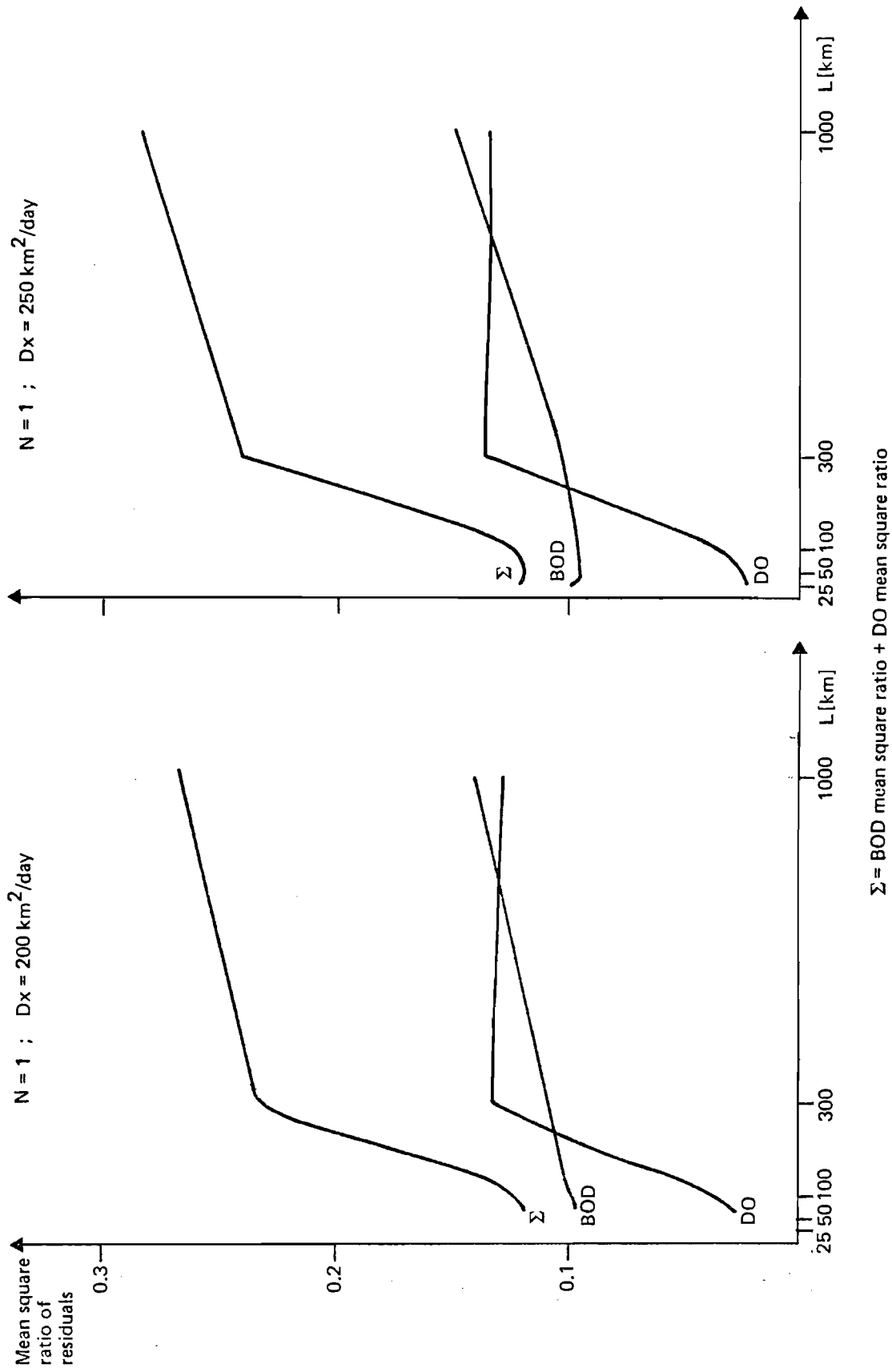


Figure 12. Quality Indexes for the River Cam, $N=1$, $D_x=200 \text{ km}^2/\text{day}$ and $D_x=250 \text{ km}^2/\text{day}$.

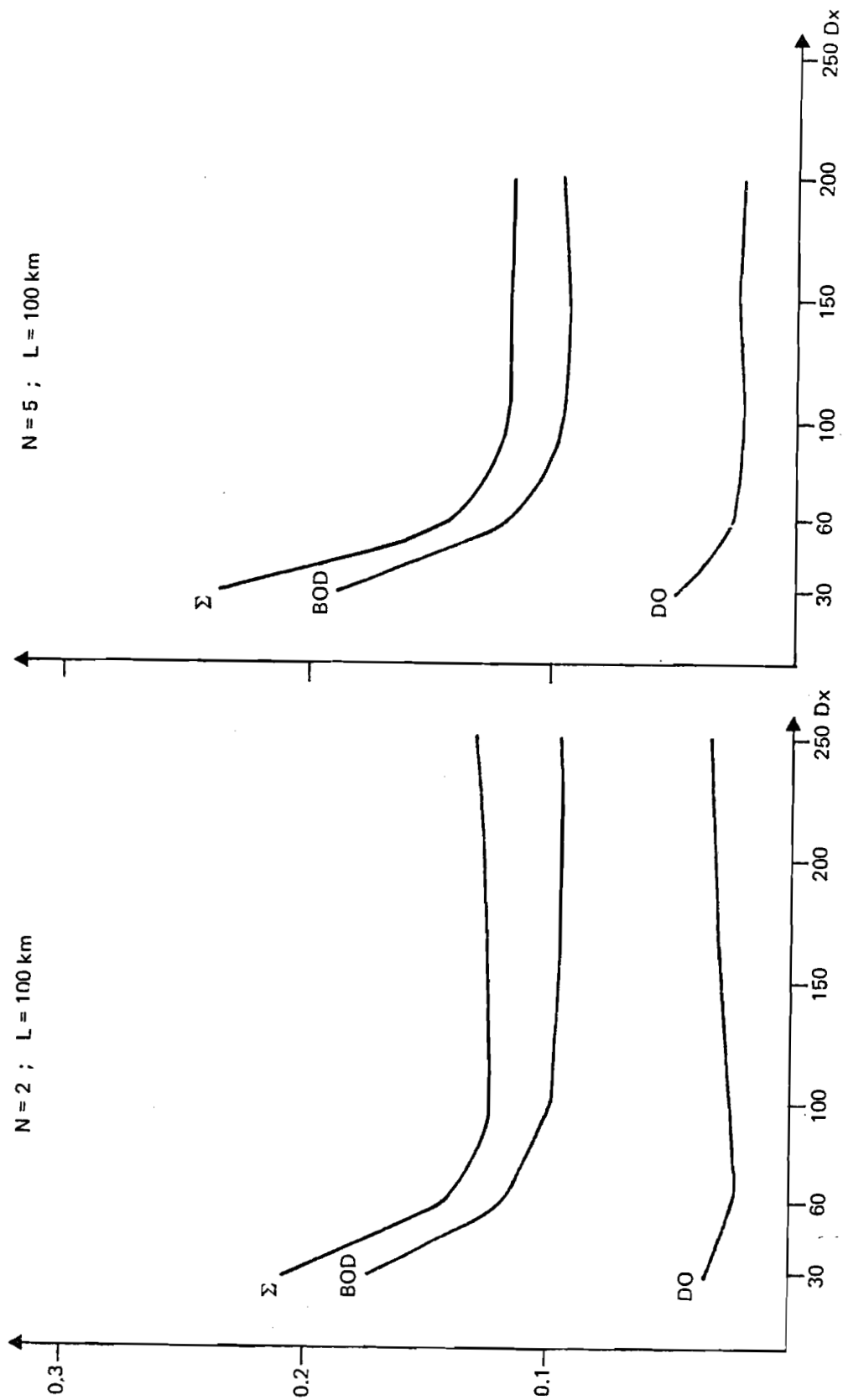


Figure 13. Quality Indexes for River Cam, N=2, L=100 km and N=5, L=100 km.

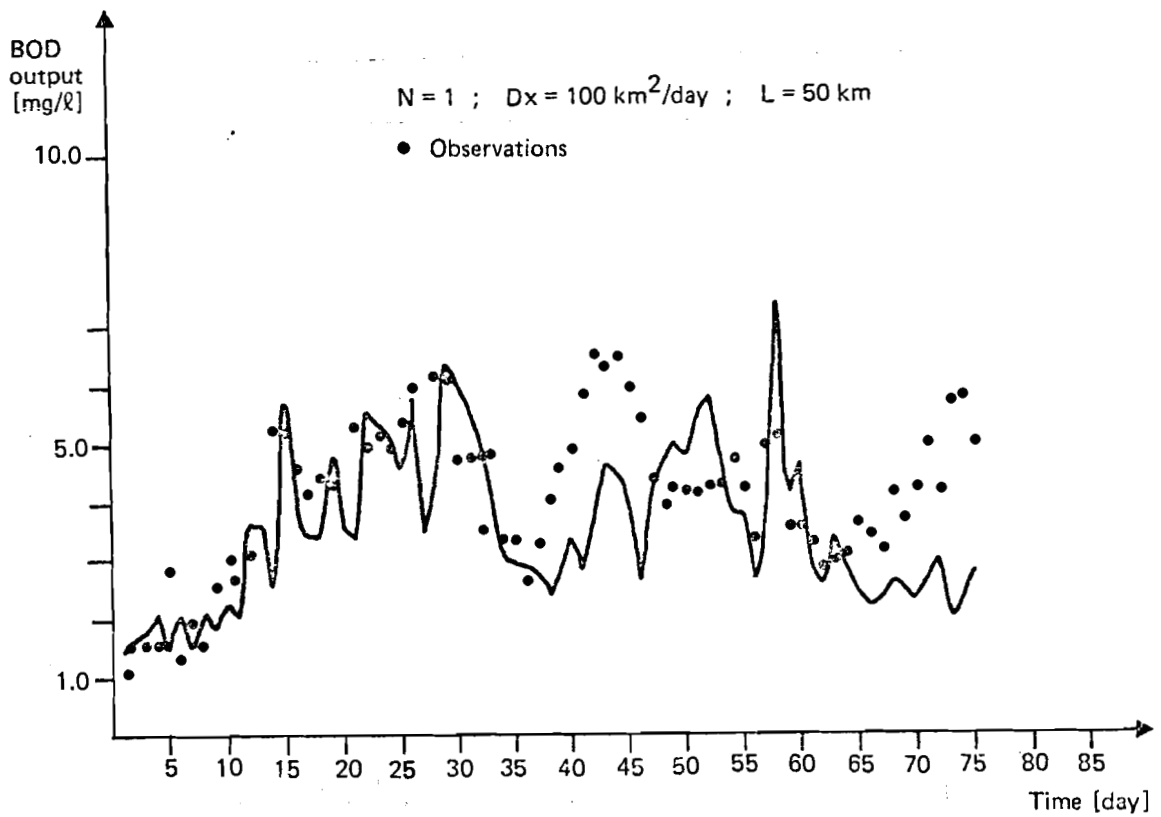
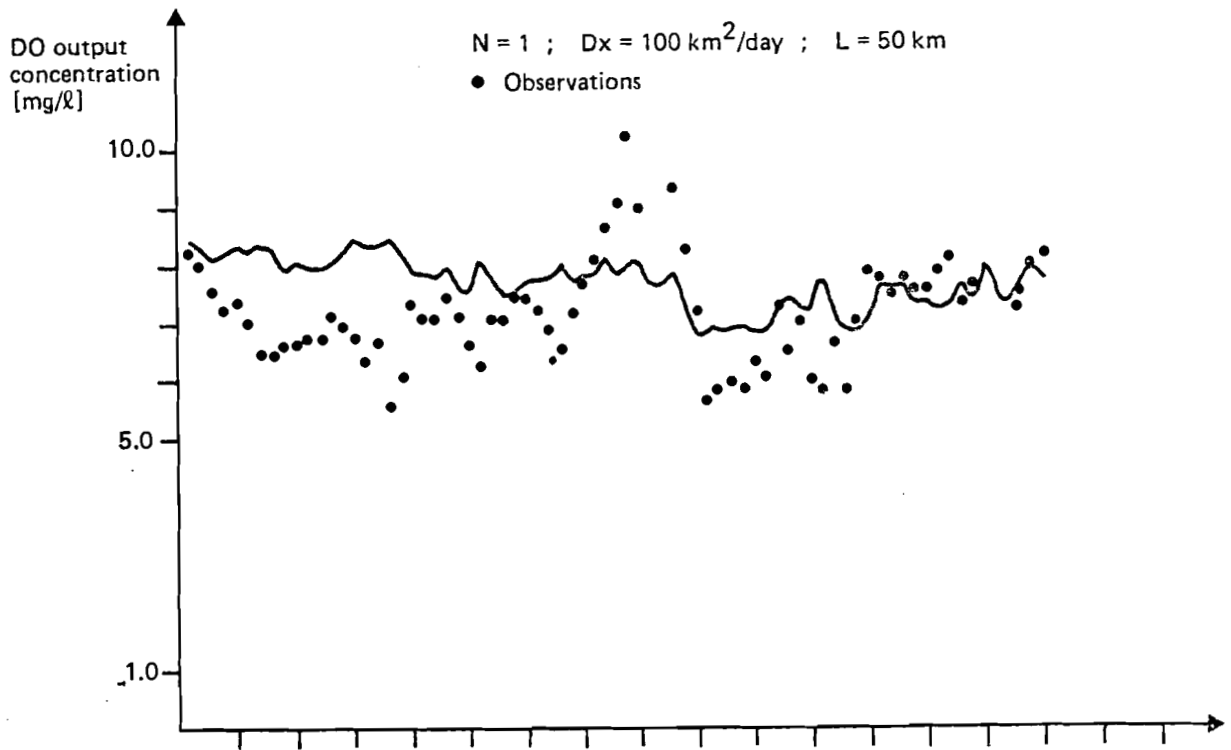


Figure 14. Input Signals of the Resulting Simplified Model for the River Cam

Table 2. Comparison of Quality Index Values for the Simplified Models

ndim	Simplified Model $D_x = 100 \text{ km}^2/\text{day}$						Model I*
	$\ell = 50 \text{ km}$			$\ell = 100 \text{ km}$			
	Static Model	1	2	1	2	3	
av.r.BOD	-0.135	-0.136	-0.142	-0.118	-0.119	-0.127	0.596
av.r.DO	0.061	0.006	0.005	0.078	0.059	0.011	0.194
m.sq.r. BOD	0.102	0.099	0.099	0.099	0.098	0.097	0.370
m.sq.r. DO	0.025	0.022	0.022	0.028	0.025	0.022	0.054

av.r.BOD = average ratio of BOD residual = average of BOD residual/average of measured BOD.

m.sq.r.BOD = mean square ratio of BOD residual = mean square of BOD residual/mean square of measured BOD.

* Beck, 1978.

It is known that using the Fourier method for approximation of the signal generates the largest error near the boundaries of the space variable, and the smallest one near the middle of this domain. Consequently, for $x = 4.5 \text{ km}$, the resulting length of the river section ought to be equal to about 10 km. On the other hand, we cannot take too small a value for ℓ , because we assumed an arbitrary right boundary condition for the PDE model (for simplicity, equal to zero). The influence of the right boundary condition would be negligible if the length ℓ taken into account is sufficiently large. It follows that the simplified model fits better for $\ell = 50 \text{ km}$ than for $\ell \approx 10 \text{ km}$ (with $x = 4.5 \text{ km}$ in the middle of the length). The question

arises why $D_x = 100 \text{ km}^2/\text{day}$ gives the best fit of the model even though it appears to be far too large a value. According to Thomann (1973), the coefficient $P = k_{11} * D_x/u^2$ characterizes quite well the main properties of the river. He proposes the following river classification:

- $P < 0.01$ for upstream feeder streams
- $0.01 < P < 0.5$ for main drainage rivers
- $0.5 < P < 1.0$ for large rivers
- $1.0 < P < 10.0$ for tidal rivers
- $P > 10.0$ for estuaries.

The Cam approximates a main drainage river, so taking k_{11} and u from Table 1 we ought to obtain the best model fit for $1 \text{ km}^2/\text{day} < D_x < 30 \text{ km}^2/\text{day}$. The value $D_x = 100 \text{ km}^2/\text{day}$ suggests that the Cam is a tidal river.

It was shown by Beck (1978) that the incorporation of "sustained sunlight effects" into the BOD and DO equations, to represent the effect of interaction of an algal population with DO and BOD dynamics, gives a significant improvement in the model responses and also in the model fit. Incorporating "sustained sunlight effects" in both equations (BOD and DO), Beck (1978) achieved the results shown in Table 3.

The simplified model described above does not include the term of "sustained sunlight effects"; although it would be easy to do so. The omission of this significant effect causes the responses of the system (especially BOD response) to be too low, compared to actual measurements. Consequently, in order to compensate for the influence of sunlight, the gain coefficient k_{sn} (see equation (47)) must be artificially

Table 3. Comparison of Quality Index Values for Beck Models

Model I		Model II*	
BOD m.sq.r.	0.370	BOD m.sq.r.	0.169
DO m.sq.r.	0.054	DO m.sq.r.	0.025

*Model with "sustained sunlight effect" incorporated

increased. This is the reason why the value of D_x is so large; when D_x increases, then the value of k_{sn} also increases especially for $n=1$ and for $D_x < 150 \text{ km}^2/\text{day}$ (see Figure 15).

To show that the above statement is valid, simulation experiments with the simplified model which indicates the effects of sunlight have been performed. It was assumed that the term representing the influence of sustained sunlight (hours of sunlight per day) has the following term:

$$k_3 \cdot S(t) \quad , \quad (65)$$

where

$S(t)$ - sunlight incident upon local area (hrs/day);

k_3 - coefficient for sustained sunlight effect, same as in the BOD and DO equations.

The term (65) has been added to the PDE equations (1), (2), consequently the term:

$$k_3 \cdot S(t) = \frac{2n\pi \cdot [1 - e^{-\hat{\alpha} \cdot \ell} \cdot (-1)^n]}{(\alpha \cdot \ell)^2 + (n\pi)^2} \quad , \quad (66)$$

has been added to the equations (41), (42).

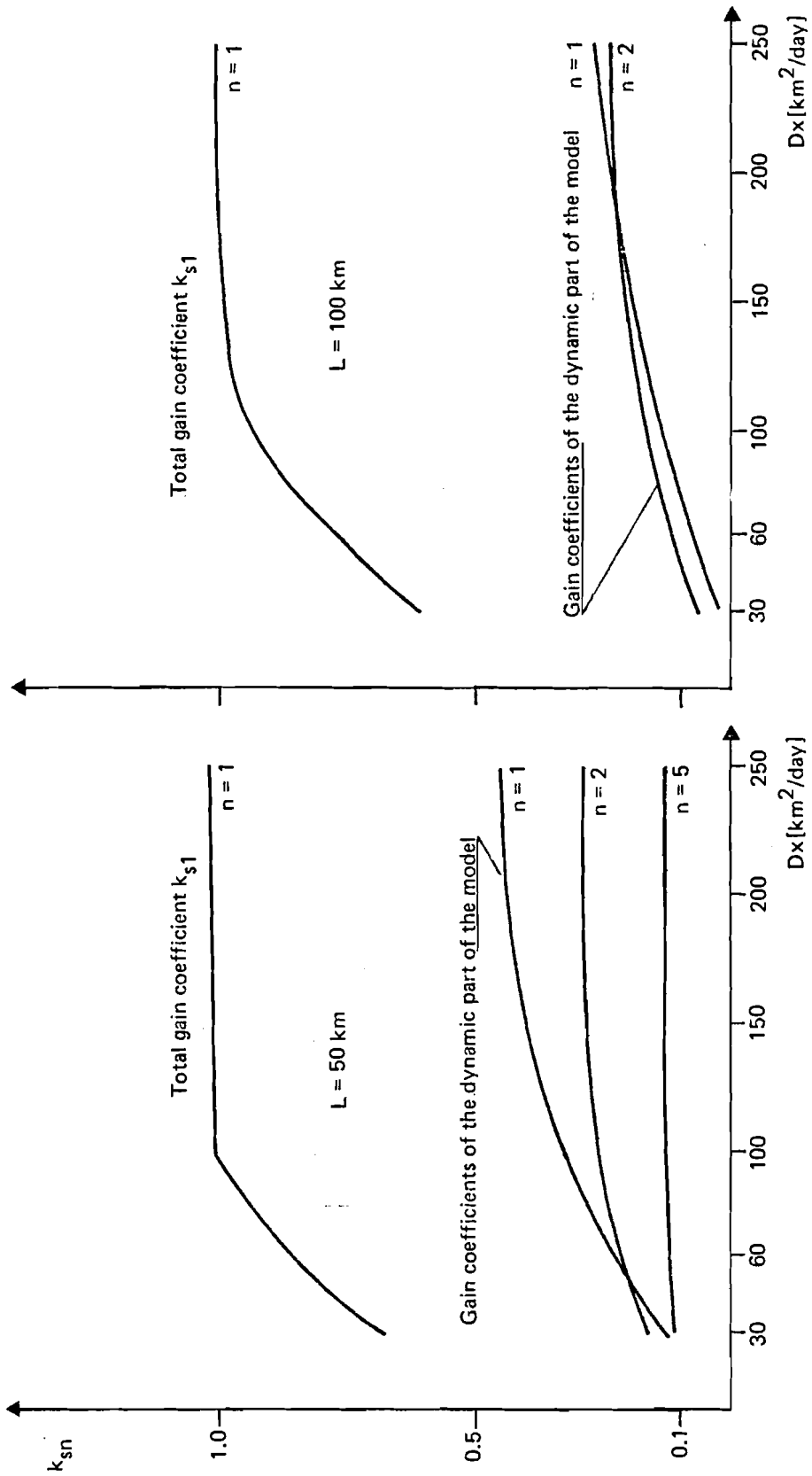


Figure 15. BOD Gain Coefficients as the Function of the Dispersion Coefficient

The results of the experiments performed for the simplified model with the sunlight effects and with the parameters taken from Table 1, are shown in Table 4.

Table 4. Quality Index Values for the Simplified Models with Sustained Sunlight Effect Incorporated

D _x [km ² / day]	Simplified Model with Sustained Sunlight Effect Incorporated						Model II [*]	
	Quality Indexes	k ₃						
		0.1	0.25	0.4	0.5	0.6		1.0
10	QV.T.BOD	-0.631	-0.565	-0.500	-0.456	-0.412	-0.238	
	QV.T.DO	-0.589	-0.548	-0.507	-0.479	-0.452	-0.342	
	m.sq.t. BOD	0.427	0.358	0.301	0.269	0.242	0.187	
	m.sq.r. DO	0.357	0.309	0.266	0.241	0.217	0.144	
20	QV.T.BOD	-0.397	-0.301	-0.204	-0.140	-0.076	-0.181	0.239
	QV.T.DO	-0.323	-0.265	-0.208	-0.169	-0.131	0.023	0.037
	m.sq.r. BOD	0.205	0.147	0.112	0.103	0.104	0.215	0.169
	m.sq.r. DO	0.119	0.085	0.059	0.049	0.041	0.055	0.025
30	QV.T.BOD	-0.286	-0.181	-0.076	-0.007	0.063	0.343	
	QV.T.DO	-0.202	-0.143	-0.085	-0.046	-0.007	0.150	
	m.sq.r. BOD	0.138	0.095	0.079	0.083	0.100	0.290	
	m.sq.r. DO	0.058	0.037	0.025	0.023	0.025	0.077	

QV.T.BOD = average ratio of BOD residual = average ratio of BOD residual/average of measured BOD.

m.sq.r.BOD = mean square ratio of BOD residual = mean square of BOD residual/mean square of measured BOD.

* Model with "sustained sunlight effect" incorporated (Beck, 1978)

It is easy to see from Table 4, that the best model fit can be obtained for $k_3 = 0.4$, $D_x = 30 \text{ km}^2/\text{day}$. In this case the values of the quality indexes are better than in the case of the model with the sustained sunlight effects incorporated as proposed by Beck (1978).

10. FREQUENCY ANALYSIS

Let us consider the input signals, i.e., BOD and DO concentrations measured at Bait's Bite lock. Using the Fourier expansion algorithm, we can determine how many harmonic components must be taken into account to obtain 50%, 75%, and 90% of the signal energy contained in the frequency band. The results of the Fourier expansion for both input signals are shown in Table 5.

On the other hand, we should consider the frequency corresponding to the first pole of the system (see equations (53), (54), and (57)). This frequency for $D_x = 30 \text{ km}^2/\text{day}$, $\ell = 50 \text{ km}$ and the values of the other parameters taken from Table 1 is equal to

$$\omega_p = 2.76 \text{ [rd/day]} \quad . \quad (67)$$

Time constants corresponding to the first two poles of the resulting model ($D_x = 30 \text{ km}^2/\text{day}$) are equal

$$\theta_s = 1.70 \text{ [day]}, \quad \theta_c = 2.27 \text{ [day]} \quad .$$

By comparing the BOD and DO (input) signal frequency bands with the frequency corresponding to the first pole of the resulting model ($D_x = 30 \text{ km}^2/\text{day}$), we can conclude that the signal frequency bands are smaller or comparable with the frequency corresponding to the first pole of the resulting model (see Figures 16 and 17). In Figures 16 and 17, the dependence of the first two poles on the values of the dispersion coefficient is shown. It can be seen

Table 5. Results of Fourier Expansion of Input Signals

Input Signal	Number of Harmonic component K	Energy % of Input Signal	T_k [day] Period of K-th component	Limit Frequency Band of Input Signal [rd/day] $\frac{2\pi}{T_k}$
	1		78	0.08
	2		39	0.16
	3		26	0.24
	.			
	.			
	.			
BOD	10	50%	7.8	0.81
	25	75%	3.12	2.01
	33	90%	2.36	2.66
DO	18	50%	4.33	1.45
	29	75%	2.69	2.34
	36	90%	2.17	2.90

that for a rather broad range of values for this coefficient $D_x < 20 \text{ km}^2/\text{day}$ or $D_x > 60 \text{ km}^2/\text{day}$, the system dynamics can be neglected; in other words, the first order model should be sufficiently accurate for $20 \text{ km}^2/\text{day} < D_x < 60 \text{ km}^2/\text{day}$. On the other hand, taking into account the results presented in Table 2, notice that the quality indexes for a static model are a little bit worse than for the simplified model with one inertia term, although they are better than quality indexes for Model I of Beck (1978).

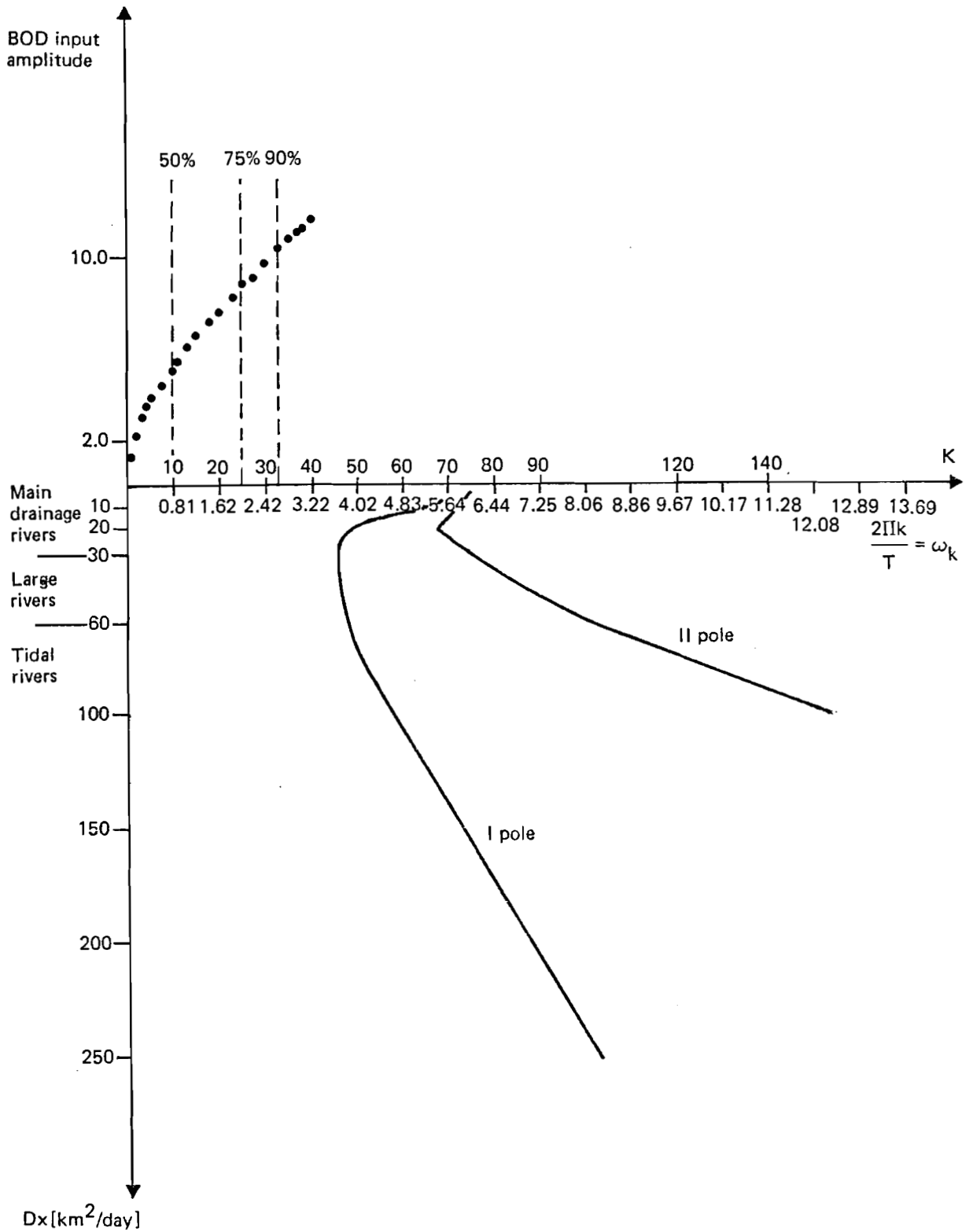


Figure 16. Comparison of BOD Input Signal Frequency Band with Frequency corresponding to the First Two Poles of the Simplified Model

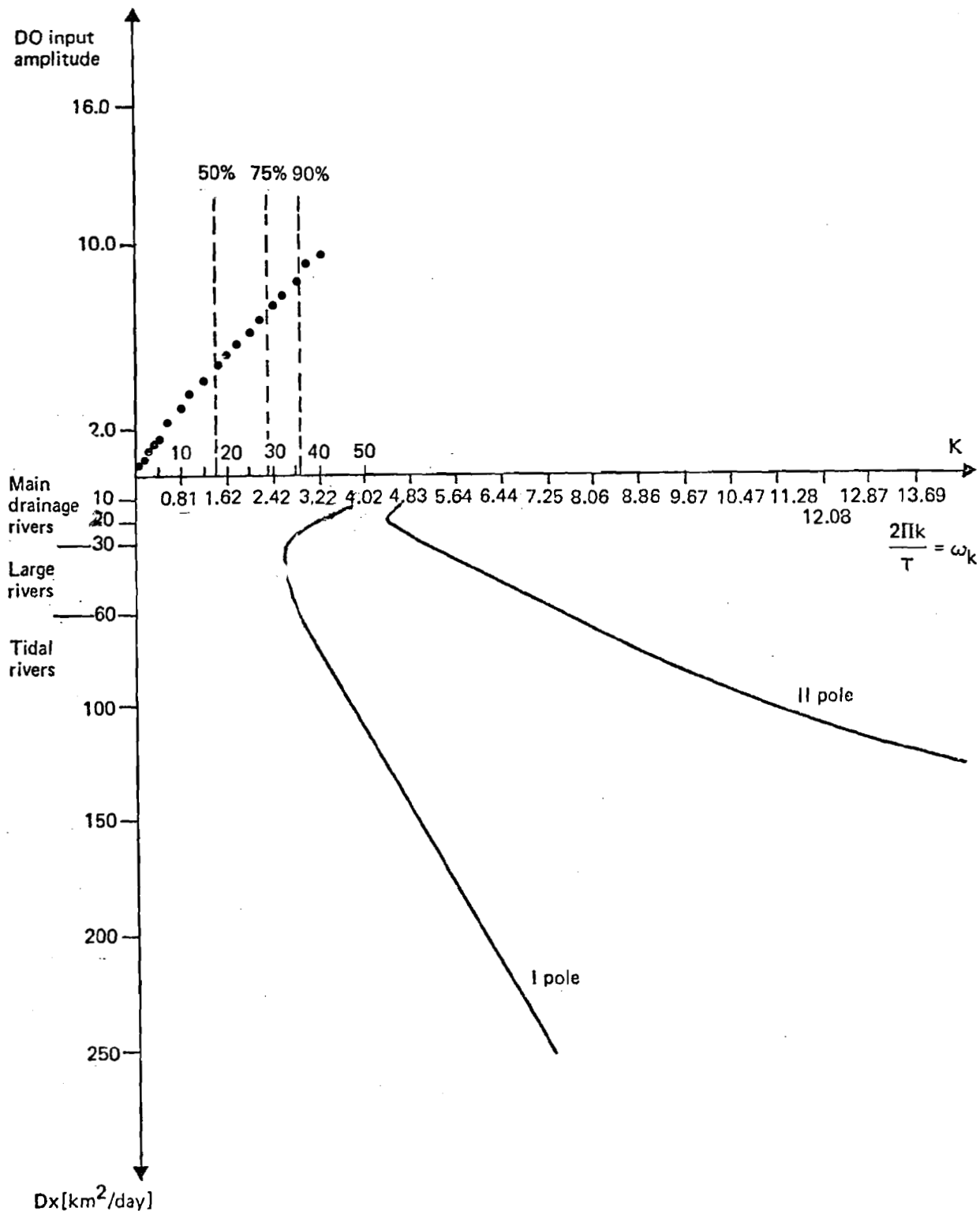


Figure 17. Comparison of DO Input Signal Frequency Band with the Frequency corresponding to the First Two Poles of the Simplified Model

Let us also compare the gain coefficient values for the dynamic part and for the proportional term of the simplified model (see Table 6). We can see that corresponding to the first two inputs, the gain coefficients are more than twice as large for the proportional terms as for the dynamic part of the model. These results illustrate the point that the proportional terms (see equations (61) and (62) have fundamental influence on model accuracy.

Compare now the models developed by Beck (1978) and the simplified model for $D_x = 30 \text{ km}^2/\text{day}$, taking into account their parameters. The results are summarized in Table 6. From this comparison, it is obvious that the gain coefficients have similar values for both models (a little bit smaller for the simplified model with $D_x = 30 \text{ km}^2/\text{day}$). The time constants are also very close, although in Model II in Beck's paper, they are a little bit smaller. The basic difference arises, however, in the shape of the frequency characteristic caused by the different structure of the models. These characteristics are schematically presented in Figure 18. The frequency characteristic of the simplified model, which in fact is the parallel connection of one inertia term and proportional term (see Figure 5) has one pole and one zero, whereas Model II in Beck's paper contains only one pole. It is necessary to point out, however, that within the frequency band of interest, these characteristics are very close.

Computation has been done using the standard version of the fourth order Runge-Kutta algorithm from the SSP library. The simulation program was written using a specialized simulation package (see Computing at IIASA No.2) specially developed for this purpose. Sums of the Fourier series have been calculated by Euler transformation, which is realized by subroutine TEUL from the SSP library.

Table 6. Comparison of Gain Coefficient Values and Time Constant Values in the Resulting Simplified Model and in Beck's Model

Inputs to BOD equation and DO equation	The Gain Coefficients in the Resulting Simplified Model $D_x = 30 \text{ km}^2/\text{day}$			The Gain Coefficients in Model II (Beck and Young, 1975)
	Dynamic Part	Proportional Terms	Resultant Gain	
BOD in BOD eq.	0.120	0.534	0.654	1.0
DO in DO eq.	0.171	0.580	0.751	1.0
BOD in DO eq.	0.087	0.247	0.334	0.378
1(t) in DO eq.	0.290	0.399	0.689	1.183
Time Constants				
θ_{BOD}		1.70		1.18
θ_{DO}		2.27		1.18

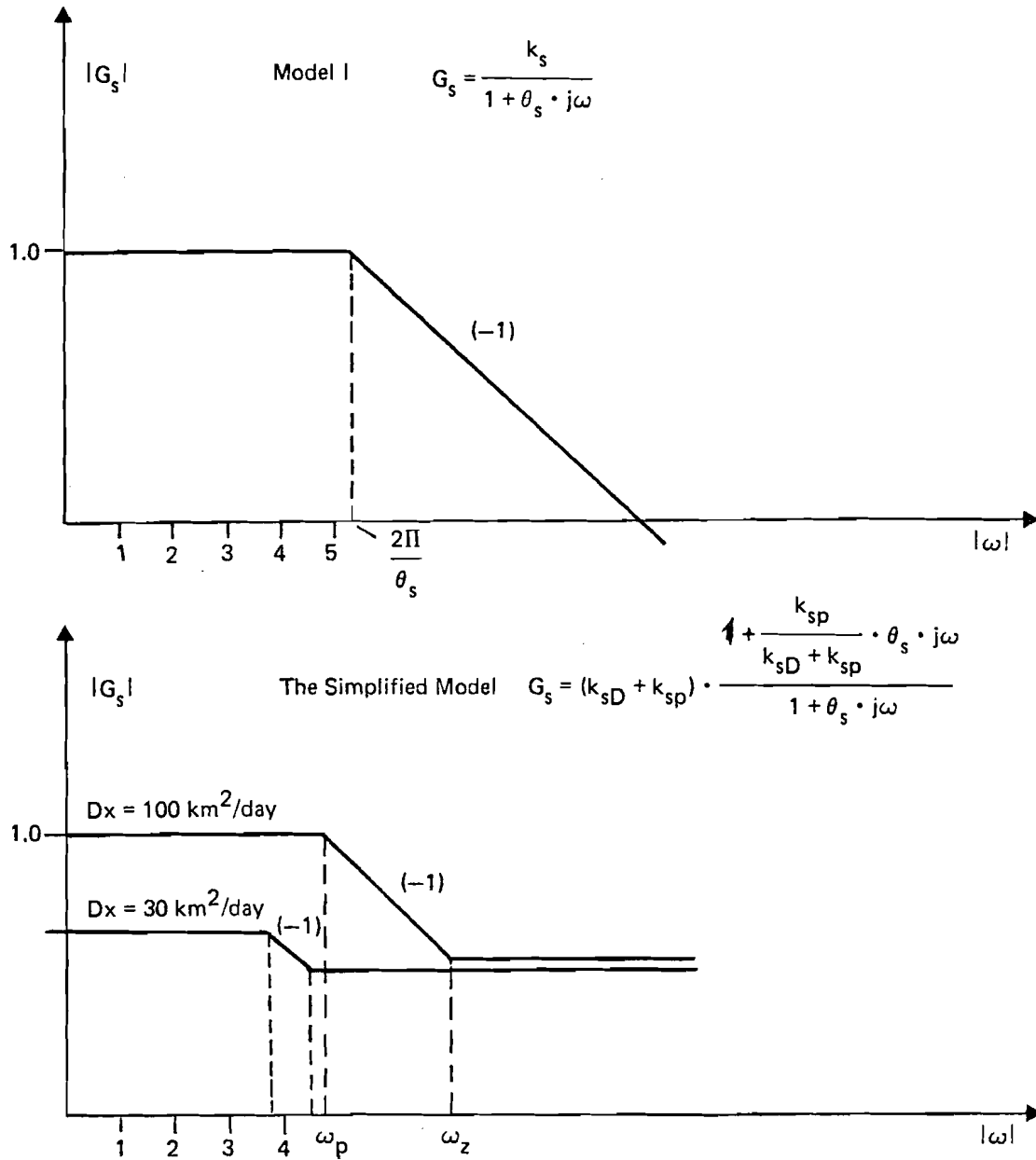


Figure 18. Frequency Characteristics for BOD Input, BOD Output Transmittances.

k_s - gain coefficient in Model I (Beck, 1978)

k_{sD} - gain coefficient of Dynamic Part of Simplified Model

k_{sp} - gain coefficient of Proportional Term of Simplified Model

θ_s - time constant.

APPENDIX

By using the separation of variables method (SVM), a linear partial differential equation of second order can be reduced to a set of ordinary differential equations. This method is described by Porter (1966) as a general case.

We then describe SVM for the diffusion equation with the constant coefficient

$$\frac{\partial s}{\partial t} = D_x \cdot \frac{\partial^2 s}{\partial x^2} + f(x,t) \quad (A1)$$

with boundary conditions,

$$s(0,t) = \psi_1(t) \quad (A2)$$

$$t \in [0, t_f]$$

$$s(l,t) = \psi_2(t) \quad (A3)$$

and initial condition,

$$s(x,0) = \alpha(x) \quad , \quad x \in [0, l] \quad . \quad (A4)$$

Consider equation (A1) with $f = 0$. A solution to this equation (auxiliary conditions) in the form

$$s(x,t) = X(x) \cdot T(t) \quad , \quad (A5)$$

is assumed to exist, when X, T are scalar valued functions of a single variable. By substituting this expression into equation (A1) with $f = 0$ and dividing it by $s(x,t)$, we obtain

$$\frac{T'(t)}{T(t)} = \frac{\ddot{X}(x)}{X(x)} \cdot D_x \quad (A6)$$

where the notation

$$T' = \frac{dT}{dt} \quad , \quad \dot{X} = \frac{dX}{dx}$$

is used.

Consider equation (A6). The left side is independent of x and the right side is independent of t . So the conclusion is that both sides are constant. Hence, for the scalar λ equation (A6) is replaced by two ordinary differential equations

$$T'(t) + D_x \cdot \lambda \cdot T(t) = 0 \quad . \quad (A7)$$

$$\ddot{X}(x) + \lambda \cdot X(x) = 0 \quad . \quad (A8)$$

If the function s satisfies auxiliary conditions, then T and X must inherit equivalent constraints. During the first stage we consider the case of homogenous boundary conditions, this means $\psi_1 = \psi_2 = 0$. The equivalent boundary conditions on X are

$$X(0) = X(\ell) = 0 \quad . \quad (A9)$$

To solve the original problem, we must locate those values $\{\lambda_n\}$ for which equations (A8), (A9) have solutions $\{X_n\}$ and

associated solutions $\{T_n\}$ for equation (A7). A linear combination $\sum C_n \cdot X_n \cdot T_n$ must be constructed to satisfy equation (A1) and the system initial conditions.

The solution of equation (A8) is given by

$$X(x) = C_1 \cdot \cos(\sqrt{\lambda}x) + C_2 \cdot \sin(\sqrt{\lambda}x) \quad . \quad (A10)$$

Taking into consideration the boundary conditions of (A9), we can compute C_1, C_2 in equation (A10). As a result we obtain $C_1 = 0$, $C_2 \neq 0$ and the eigenvalues are equal to

$$\lambda_n = \left(\frac{n \cdot \Pi}{\ell}\right)^2, \quad n = 1, 2, \dots \quad (A11)$$

The eigenfunctions being the solutions for equations (A8), (A9) are of the following form

$$X_n(x) = C_2 \sin\left(\frac{n \cdot \Pi x}{\ell}\right), \quad n = 1, 2, \dots \quad (A12)$$

It is easy to notice that the eigen-functions of (A12) create the orthogonal basis in the $L_2(0, \ell)$ space (for simplicity we can assume $C_2 = 1$).

Each function

$$s_n(x, t) = T_n(t) \cdot \sin\left(\frac{n \cdot \Pi x}{\ell}\right), \quad n = 1, 2, \dots \quad (A13)$$

satisfies equation (A1) with boundary conditions (A2), (A3).

From the linearity of problem (A1) it follows, that the function

$$s(x, t) = \sum_{n=1}^{\infty} T_n(t) \cdot \sin\left(\frac{n \cdot \Pi \cdot x}{\ell}\right) \quad (A14)$$

can also satisfy equation (A1) with the conditions in (A2), (A3), (A4), if the expansion in (A14) converges.

Notice that equation (A14) represents a Fourier series expansion (in x) for the function $s(x,t)$. The coefficients of this expansion have the form

$$T_n(t) = \frac{2}{\ell} \int_0^{\ell} s(x,t) \cdot \sin\left(\frac{n \cdot \pi \cdot x}{\ell}\right), \quad n=1,2,\dots \quad (\text{A15})$$

Integrating the right side of equation (A15) by parts, we obtain

$$T_n(t) = \frac{2}{n \cdot \pi} \cdot [\psi_1(t) - \psi_2(t) \cdot (-1)^n] + \frac{2}{n \cdot \pi} \int_0^{\ell} \frac{\partial s}{\partial x} \cdot \cos\left(\frac{n \pi x}{\ell}\right) dx \quad (\text{A16})$$

for $n=1,2,\dots$

Once more, integrating

$$\int_0^{\ell} \frac{\partial s}{\partial x} \cdot \cos\left(\frac{n \pi x}{\ell}\right) dx$$

by parts, we obtain

$$\int_0^{\ell} \frac{\partial s}{\partial x} \cdot \cos\left(\frac{n \pi x}{\ell}\right) dx = - \frac{\ell}{n \cdot \pi} \int_0^{\ell} \frac{\partial^2 s}{\partial x^2} \cdot \sin\left(\frac{n \pi x}{\ell}\right) dx \quad (\text{A17})$$

for $n=1,2,\dots$

Now we can compare equation (A17) and equation (A16)

$$T_n(t) = \frac{2}{n \pi} \cdot [\psi_1(t) - \psi_2(t) \cdot (-1)^n] - \frac{2 \cdot \ell}{n^2 \pi^2} \int_0^{\ell} \frac{\partial^2 s(x,t)}{\partial x^2} \cdot \sin\left(\frac{n \cdot \pi \cdot x}{\ell}\right) dx \quad (\text{A18})$$

for $n=1,2,\dots$

Comparing equations (A18) and (A1) we conclude that

$$T_n(t) = \frac{2}{n \cdot \Pi} \cdot [\psi_1(t) - \psi_2(t) \cdot (-1)^n] - \frac{2 \cdot \ell}{n^2 \Pi^2} \int_0^\ell \frac{1}{D_x} \left[\frac{\partial s}{\partial t} - f(x,t) \right] \cdot \sin\left(\frac{n\Pi x}{\ell}\right) dx, \quad n=1,2,\dots \quad (A19)$$

Differentiating equation (A15) in t we get

$$\frac{dT_n}{dt} = \frac{2}{\ell} \int_0^\ell \frac{\partial s}{\partial t} \cdot \sin\left(\frac{n\Pi x}{\ell}\right) dx, \quad n=1,2,\dots \quad (A20)$$

From a comparison of equations (A19) and (A20) it follows that expansion coefficient $T_n(t)$ must satisfy the following equation:

$$\begin{aligned} \frac{d}{dt} T_n(t) + \left(\frac{n \cdot \Pi}{\ell}\right)^2 \cdot D_x \cdot T_n(t) &= \frac{2 \cdot n \cdot \Pi}{\ell^2} \cdot D_x \cdot \\ &\cdot [\psi_1(t) - \psi_2(t) \cdot (-1)^n] + f_n(t), \quad n=1,2,\dots \end{aligned} \quad (A21)$$

where

$$f_n(t) = \frac{2}{\ell} \int_0^\ell f(x,t) \cdot \sin\left(\frac{n\Pi x}{\ell}\right) \cdot dx, \quad n=1,2,\dots \quad (A22)$$

The initial conditions can be obtained in a similar way

$$T_n(0) = \frac{2}{\ell} \int_0^\ell \Phi(x) \cdot \sin\left(\frac{n \cdot \Pi \cdot x}{\ell}\right) dx, \quad n=1,2,\dots \quad (A23)$$

Summarizing, the infinite set of ordinary differential equations (A21) together with the initial conditions is equivalent to the distributed-parameter boundary-value problem (A1)-(A4).

REFERENCES

- Beck, M.B. 1978. A Comparative Case Study of Dynamic Models for DO-BOD-Algae Interaction in a Freshwater River, RR.78-19, December. International Institute for Applied Systems Analysis, Laxenburg, Austria.
- Beck, M.B. 1980. Model Structure Identification from Experimental Data, RR-80-4, February. International Institute for Applied Systems Analysis, Laxenburg, Austria.
- Beck, M.B., and P.C. Young. 1975. A Dynamic Model for DO-BOD Relationships in a Non-tidal Stream, Water Res., 9, pp. 769-776.
- Jenkins, G.M., and D.G. Watts. 1968. Spectral Analysis and its Applications, San Francisco, USA.
- Porter, W.A. 1966. Modern Foundations of Systems Engineering, Macmillan Company, New York, USA.
- Raibman, N.S., and V.M. Chadeev. 1975. Modeling of Industrial Processes Moskva, Energiya, USSR.
- Rinaldi, S., R. Soncini-Sessa, H. Stehfest, and H. Tamura. 1979. Modeling and Control of River Quality, McGraw Hill.
- Thomann, R.V. 1972. Systems Analysis and Water Quality Management, McGraw Hill.
- Thomann, R.V. 1973. Effect of Longitudinal Dispersion on Dynamic Water Quality Response of Streams and Rivers, Water Resources Research, Vol. 9, No. 2, April.
- Tikhonov, A.N., and V.Y. Arsenin. 1977. Solutions of Ill-Posed Problems, New York.
- Vasiliev, O.F. 1979. Mathematical Modeling of Water Quality in River Channels and its Systems, WP-79-121, December. International Institute for Applied Systems Analysis, Laxenburg, Austria.